Volume 12 | Number 14 | 21 July 2025

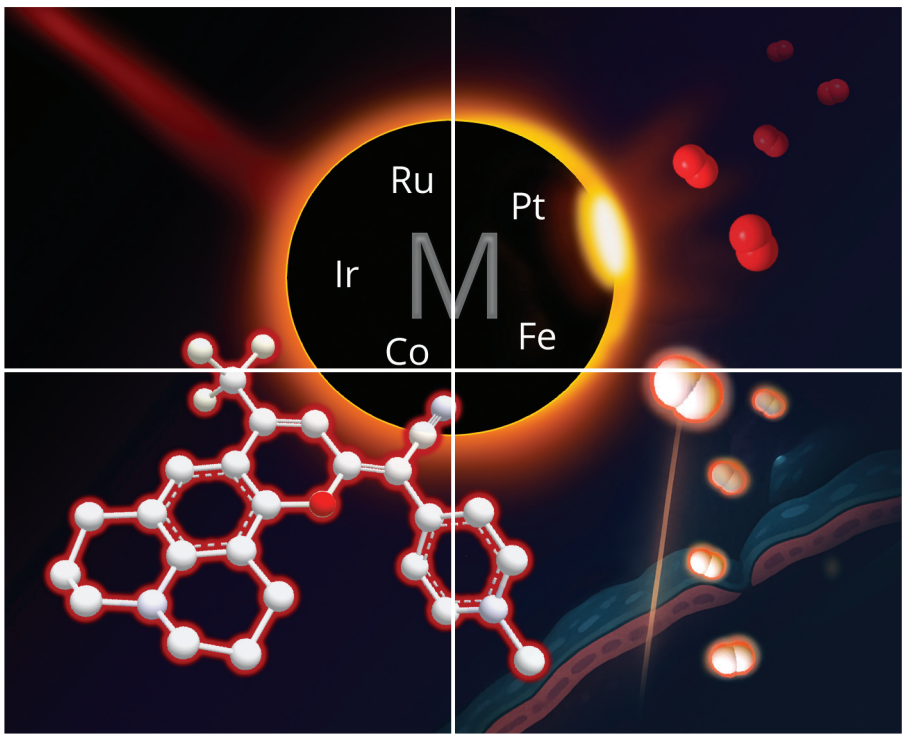

INORGANIC CHEMISTRY

FRONTIERS

CCS 中国化学会 CHINESE CHEMICAL SOCIETY
PEKING UNIVERSITY 1898
ROYAL SOCIETY OF CHEMISTRY
rsc.li/frontiers-inorganic

INORGANIC CHEMISTRY FRONTIERS

REVIEW

View Article Online
View Journal | View Issue

Cite this: *Inorg. Chem. Front.*, 2025, **12**, 4355

Metal–coumarin derivatives as promising photosensitizers: unlocking their cancer phototherapy potential†

Gloria Vigueras, [a] Eduardo Izquierdo-García, [b] Elena de la Torre-Rubio, [b] Diego Abad-Montero, [b] Maria Dolores Santana, [a] Vicente Marchán *[b] and José Ruiz *[a]

The coumarin scaffold exhibits remarkable chemical adaptability, allowing modifications at nearly every position. This versatility enables precise customization of its photophysical, photochemical, physicochemical, and biological properties both for bioimaging and therapeutic applications. Transition metal complexes with photofunctional capabilities have also garnered significant attention as light-activated drugs due to their diverse and well-established photophysical and photochemical characteristics, facilitating numerous biomedical applications. In this context, both coumarin derivatives and transition metal complexes have been extensively employed in light-induced therapies, including photodynamic therapy (PDT) for cancer treatment. PDT, a clinically approved treatment modality for various medical conditions, relies on the use of light-activated drugs, known as photosensitizers (PSs), which are activated by specific wavelengths of light to generate cytotoxic reactive oxygen species (ROS) capable of eliminating cancer cells. This review offers a comprehensive analysis of the strategic development of advanced metal-based PSs incorporating coumarin derivatives, emphasizing the unique photophysical, photochemical and photobiological properties provided by the coumarin scaffold. The discussion is systematically divided into two major sections based on the integration approach of the coumarin within the metal complexes: 1. metal complexes with coumarin attached *via* non-conjugated linkers. This section details cases where coumarin is indirectly linked to the metal center. 2. Metal complexes with coumarin integrated into ligands. This section explores systems where the coumarin is directly involved in the metal coordination sphere, either through direct bonding or *via* conjugated linkers that enhance electronic interactions with the metal center. This structured approach facilitates an in-depth comparison and analysis of design strategies for these innovative therapeutic agents. Special attention is given to metal–COUPY conjugates, featuring cyclometalated Ir(III) or Ru(II) complexes, and Ru(II)–COUBPY complexes, where the coumarin scaffolds are incorporated into Ru(II) polypyridyl complexes through a bipyridine ligand.

Received 27th March 2025,
Accepted 4th May 2025

DOI: 10.1039/d5qi00858a

rsc.li/frontiers-inorganic

I. Introduction

a. Coumarins: general structure and biological relevance

Coumarins derive their name from "Coumarou", the French name for the tonka bean (Dipteryx odorata Willd., Fabaceae), from which the simplest coumarin was first isolated in 1820. These aromatic compounds belong to the benzopyrone family, characterized by a benzene ring fused to a pyrone moiety (Fig. 1). The coumarin scaffold is widely found in numerous plants, as well as in certain fungi and bacteria, where it is biosynthesized as a secondary metabolite, primarily *via* the shikimic acid pathway. In recent years, both naturally occurring coumarins and their synthetic derivatives have garnered increasing attention due to their broad range of biological activities, largely attributed to their ability to interact with various enzymes and molecular targets in living systems.[1] Coumarin-based compounds are widely used as pesticides,[2] food additive,[3] perfumes and cosmetics,[4] allelopathic agents,[5] anticancer and antibacterial agents,[6,7] anticoagulants,[8] and in various other industrial and therapeutic applications.[9]

The numbering of coumarin atoms starts from the lactone oxygen, which is assigned as number 1, increasing consecu-

[a]*Departamento de Química Inorgánica, Universidad de Murcia, Biomedical Research Institute of Murcia (IMIB-Arrixaca), E-30100 Murcia, Spain. E-mail: jruiz@um.es*
[b]*Departament de Química Inorgànica i Orgànica, Secció de Química Orgànica, Universitat de Barcelona (UB), Institut de Biomedicina de la Universitat de Barcelona (IBUB), Martí i Franquès 1-11, E-08028 Barcelona, Spain. E-mail: vmarchan@ub.edu*

† Electronic supplementary information (ESI) available. See DOI: https://doi.org/10.1039/d5qi00858a

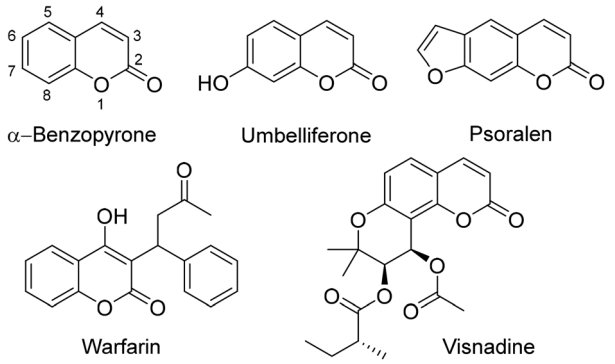

Fig. 1 Representative examples of coumarins with therapeutic applications.

tively as shown in Fig. 1. The structure of the coumarin can be easily modified, allowing for the fine-tuning of their physicochemical and biological properties through the incorporation of different substituents at key positions of the backbone. Various synthetic approaches, such as the Pechmann, Knoevenagel, and Perkin reactions, have been employed for the synthesis and functionalization of a wide variety of coumarin derivatives.[10] Coumarins can be broadly classified into four main categories: simple coumarins, pyrone-substituted coumarins, furanocoumarins and pyranocoumarins. Simple coumarins are characterized by the presence of alkyl, alkoxy, hydroxyl or amino substituents on the benzene ring, with **Umbelliferone** serving as a representative example. Furanocoumarins such as **Psoralen** consist of a five-membered furan ring fused to the benzene ring and are typically used in the treatment of skin diseases through psoralen-based photochemotherapy (PUVA).[11] **Visnaline**, is a representative example of a pyranocoumarin containing a six-membered pyran ring fused to the benzene ring exhibiting analgesic and anti-inflammatory properties.[12,13] Lastly, pyrone-substituted coumarins are distinguished by the functionalization of the pyrone moiety at either the third or fourth carbon position, with **Warfarin** being widely used as an anticoagulant drug.

The coumarin scaffold exhibits exceptional chemical versatility, allowing for modifications at almost any position. This flexibility enables precise tailoring of its photophysical, photochemical, physicochemical, and biological properties to suit specific applications. Among their diverse applications, coumarin derivatives are particularly notable as organic fluorophores due to their relatively high fluorescence quantum yields, large Stokes' shifts, and excellent cell membrane permeability.[14] Coumarin-based fluorophores (CBFs) are invaluable tools in the fields of sensing and molecular detection. For example, they can be used for the detection of inorganic ions, as well as amino acids and peptides.[15–17] CBFs have also been applied for pH and microenvironment polarity detection, serving as fluorescent probes for materials and fluorescent labels for bioimaging.[18]

While the original 2*H*-chromen-2-one structure exhibits limited fluorescence, CBFs' absorption and emission spectrum can be fine-tuned through strategic backbone modifications. A key approach in designing new CBFs involves the introduction of electron-donating groups (EDG) at position 7 (*e.g.* hydroxyl, alkoxy or *N*,*N*-dialkylamino substituents) that partner with the electron-withdrawing lactone to create a push–pull effect along the π system, but also electron-withdrawing groups (EWG) at positions 3 or 4 (*e.g.* trifluoromethyl, ester, or cyano groups), which can also induce a red-shift in absorption and emission maxima. Expanding the π-conjugation system represents another widely used strategy for tuning optical properties of the coumarin scaffold, often achieved by incorporating polymethine bridges or bulky aromatic moieties through position 3, including the attachment of other organic fluorophores such as pyrene, hemicyanine, or BODIPY.[19–22]

Despite huge synthetic efforts dedicated to the coumarin scaffold, little work has been devoted to modifying the lactone function to develop new CBFs. As shown in Fig. 2, both the thionation of the carbonyl group[23] and the incorporation of a dicyanomethylene group[24,25] have been described to cause significant red-shift in the 7-*N*,*N*-diethylamino series compared to the original coumarin, leading to green light emission. In 2018, Marchán *et al.* were pioneers in describing a new family of CBFs, named COUPYs, that arise from the incorporation of a cyano(1-alkyl-4-pyridin-1-ium)methylene motif at the 2-position of the coumarin backbone. This structural modification endows COUPY dyes with tunable photophysical properties, including far-red and near-infrared (NIR) emission and large Stokes' shifts (Fig. 2).[26–29] COUPY dyes inherently accumulate in mitochondria owing to their positively-charged *N*-alkylpyridinium moiety, and have been successfully used to fluorescently label peptides[30] and lipids.[31] Additionally, as described in the following sections of this review, COUPY fluorophores show great potential as phototherapeutic agents, whether in their free form,[32] nanoencapsulated[33] or when conjugated and/or integrated with transition metal complexes.[34–39]

b. Photodynamic therapy (PDT)

Photodynamic therapy (PDT) is a clinically approved treatment for various medical conditions. It is particularly effective for pre-cancerous lesions of the skin and esophagus, and is also used to treat advanced cancers in the head, neck, bladder, prostate and lungs.[40,41] PDT involves the use of a photosensitizer (PS) drug that, when exposed to a specific wavelength of light, produces a variety of cytotoxic reactive oxygen species (ROS) that are capable of destroying cancer cells. This therapy is minimally invasive and can be repeated multiple times at the same site if necessary. This makes PDT a flexible and patient-friendly option for treating various conditions, as it allows for ongoing treatment without significant discomfort or recovery time. The molecular design of the PS plays a critical role in the efficacy of PDT, as key factors such as photoactivation wavelength, ROS generation efficiency, photostability, cellular uptake, biodistribution and dark toxicity directly influence treatment outcomes. Optimizing these parameters ensures that the PS can effectively target and destroy cancer cells while minimizing damage to surrounding healthy tissues. From a mechanistic point of view, the PS, upon

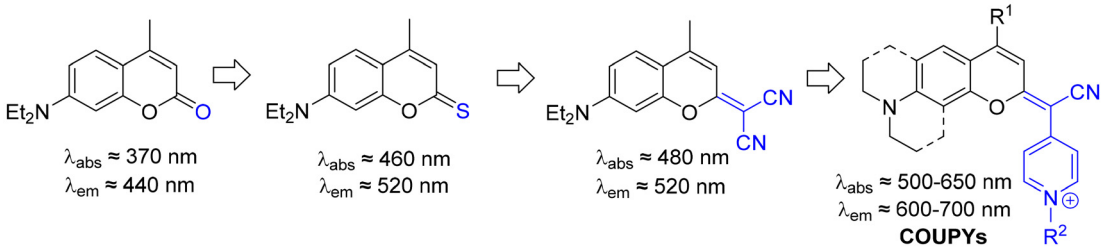

Fig. 2 Rational design of COUPY fluorophores.

exposure to light, transitions to a triplet excited state (^{3}PS*). In this state, the PS can either transfer an electron (type I PDT) or energy (type II PDT) to molecular oxygen within the targeted tissues (Fig. 3), leading to the formation of ROS that can induce three main therapeutic effects: (i) direct oxidative damage to cancer cells by affecting nucleic acids, proteins, and lipid membranes; (ii) vascular damage that depletes oxygen and induces hypoxia; and (iii) activation of the immune response.[42] The combined mechanisms contribute to PDT's strong anticancer efficacy while minimizing undesired side effects, making it an increasingly popular and well-researched therapeutic approach.

From a chemical perspective, PSs are generally classified into two main categories: organic and metal-based. Among organic PSs, coumarin derivatives have attracted considerable attention due to their structural versatility and the ease with which their photophysical and photochemical properties can be tuned. Other major families include PSs based on the tetrapyrrolic scaffold (*e.g.* porphyrins, chlorins and phthalocyanines), BODIPY dyes, xanthenes, cyanines, and phenothiazines. Interestingly, some coumarins, porphyrins, and chlorins are of natural origin, underscoring the vital role of nature-derived scaffolds in the design of modern phototherapeutic agents.[43] A key limitation of organic PSs is their relatively low efficiency in undergoing intersystem crossing (ISC) to access the triplet excited state, particularly when compared to their metal-based counterparts. Traditionally, this challenge has been addressed by incorporating heavy atoms (*e.g.*, bromine or iodine) into the molecular structure to enhance ISC *via* the "heavy atom effect". More recently, however, increasing attention has been directed toward the development of heavy-atom-free organic PSs that facilitate ISC through alternative strategies, such as spin–orbit charge transfer or twisted π-conjugation.[44] These approaches offer promising avenues for achieving efficient triplet state generation while reducing potential toxicity and improving biocompatibility.

Hypoxia is a hallmark of solid tumors, resulting from rapid cancer cell proliferation and inadequate vascularization.[45] While normal tissues maintain oxygen levels between 40–60 mmHg, many solid tumors experience levels below 10 mmHg.[46] This oxygen deficiency triggers adaptive responses, that promote tumor survival, angiogenesis, metastasis, and therapy resistance, ultimately driving disease progression, recurrence, and poor patient outcomes.[47] One of the major limitations of currently marketed PSs is their reduced efficiency in generating ROS within the hypoxic tumor microenvironment. This is because most of them primarily operate through the type II mechanism, which is highly dependent on oxygen concentration. To overcome this limitation, two key strategies have been explored: (i) developing PSs that operate through both type I and type II mechanisms, which enables the generation of ROS other than singlet oxygen ($^1O_2$), such as superoxide ($^{\bullet}O_2^-$) and hydroxyl ($^{\bullet}OH$) radicals, even under low-oxygen conditions;[48,49] (ii) integrating oxygen-releasing systems to locally increase oxygen availability.[50,51] More recently, a type III PDT mechanism has been proposed, in which the PS can directly damage biological molecules even in the absence of oxygen.[52,53]

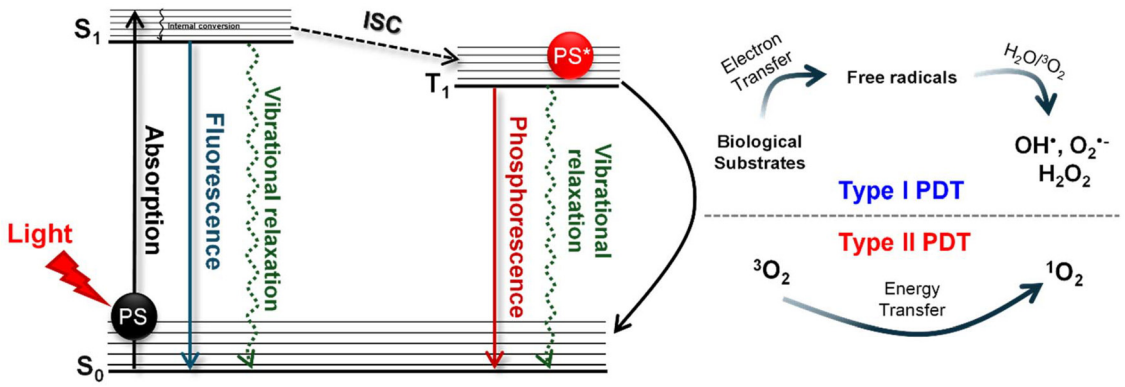

Fig. 3 Jablonski diagram illustrating type I and type II mechanisms of PDT.

c. Coumarins as PSs in PDT

Coumarins have been widely used in light-induced therapies due to their optimal photophysical properties and high biocompatibility. The strong fluorescence and high photostability of certain coumarin derivatives, combined with their ability to photogenerate ROS, make them promising candidates for PDT. As previously indicated, psoralens have been exploited in PUVA therapy for treating various skin conditions, such as psoriasis, vitiligo, and cutaneous T-cell lymphoma. In PUVA therapy, psoralens are administered either topically or orally, and then the affected skin is exposed to UVA light.[54,55] While both PUVA and PDT involve light-activated treatments, they differ significantly in their mechanisms and applications. PUVA uses psoralens and UVA light (320–400 nm) as the light source. In contrast, PDT employs various families of PSs (*e.g.*, porphyrins, chlorins, phthalocyanines or metal complexes) that are activated by longer wavelengths of light (>400 nm). Furthermore, the main mechanism of PUVA involves DNA cross-linking through photoinduced [2 + 2] cycloaddition reactions, which inhibit cell division, while PDT induces direct oxidative damage to cellular components through the generation of ROS.

In PDT, ROS generated during PS irradiation are highly reactive and short-lived, with lifetimes ranging from 0.03 to 0.18 μs in biological environments. These ROS also have limited diffusion distances (0.01–0.02 μm) within cells. Therefore, the precise subcellular localization of the PS is crucial for maximizing its phototoxic effects and ensuring effective treatment outcomes.[56] As a result, extensive efforts have been focused on developing organelle-targeted PSs to enhance PDT efficiency by directing ROS generation to critical organelles such as mitochondria, lysosomes, endoplasmic reticulum and lipid droplets.[57] In 2021, the groups of Marchán and Ruiz reported the therapeutic applications of COUPY coumarins in the context of anticancer PDT.[32] The (photo)cytotoxicity of 15 COUPY derivatives was assessed in cancerous (HeLa, A2780) and non-cancerous (CHO, BGM) cell lines, enabling the establishment of structure–activity relationships (SAR) and the identification of three lead compounds (**Cou1–3**, Fig. 4). Among them, **Cou3** exhibited the highest phototoxic activity against HeLa cells upon visible-light irradiation, under both normoxic (IC_{50}^{dark} = 2.0 ± 0.3 μM, IC_{50}^{light} = 0.028 ± 0.004 μM, PI = 71.4) and hypoxic (IC_{50}^{dark} = 17 ± 3 μM, IC_{50}^{light} = 0.56 ± 0.09 μM, PI = 30.4) conditions, while demonstrating preferential toxicity toward cancer cells over non-cancerous cells. Confocal microscopy confirmed the selective mitochondrial accumulation of COUPY derivatives, driven by their positively charged pyridinium moiety, while flow cytometry validated the ability of **Cou3** to induce mitochondrial depolarization. Mechanistic studies identified ROS generation as the primary cytotoxic mechanism under light irradiation, with peroxyl radicals ($ROO^{\bullet}$) prevailing under normoxia and singlet oxygen ($^1O_2$) under hypoxia, ultimately triggering apoptosis and/or autophagy as the main cell death pathways.

In a later study, the same groups further enhanced the PDT performance of **Cou3** by employing a pH-responsive polyurethane–polyurea hybrid nanocapsule formulation.[33] This strategy improved tumor targeting, photostability, ROS generation, and *in vitro* phototoxicity against HeLa cells upon red light irradiation while reducing dark toxicity, leading to significantly higher phototoxicity index (PI) values compared to the free compound (255 for **NC-Cou3** *vs.* 30 for **Cou3**). Notably, **NC-Cou3** displayed a notable growth inhibitory effect against HeLa multicellular tumor spheroids (MCTSs) when subjected to red light (630 nm, 89 mW cm^{-2}, 30 min), highlighting its antitumoral potential in a clinically relevant model.

Zhao *et al.* reported a series of coumarin dyes, where a cyano(*N*-alkyl-4-pyridinium)methylene motif was attached to the C3 position of the coumarin backbone *via* an alkene bridge, instead of the 2-position as seen in the COUPY dyes.[58] Among them, **Cou4** exhibited moderate *in vitro* phototoxicity against HeLa and CT-26 cells ($IC_{50}^{light} \approx 10$ μM) under white light irradiation, although it was found to inhibit tumor growth in a murine subcutaneous tumor model of CT-26 cells (Fig. 4). Coumarins have also been conjugated with other chromophores to develop novel PSs with enhanced photobiological properties, being **Cou5–Cou10** some representative examples.[59–62]

d. Role of metal complexes in phototherapy. Scope and objectives of this review

Transition metal complexes with photofunctional properties have gained considerable interest as PSs due to their rich photophysical and photochemical characteristics, which enable applications in bioimaging and therapeutic contexts, including PDT.[53,63–66] Metal complexes may offer several advantages over conventional organic PSs. The incorporation of a heavy metal center enhances spin–orbit coupling (SOC), which promotes intersystem crossing (ISC) and facilitates the efficient formation of triplet excited states, leading to high quantum yields for ROS generation. Additionally, these compounds demonstrate excellent photostability, allowing for effective ROS production at low concentrations while minimizing systemic toxicity and post-treatment photosensitivity. The structural versatility and synthetic tunability of metal complexes enable precise control over their photophysical properties and biological activity through careful selection of the metal center and ligands.[53] Due to these unique benefits, transition metal complexes have rapidly advanced as potential PSs for PDT in cancer treatment. Notably, the Ru(II) polypyridyl complex TLD1433 has shown significant promise and has reached phase II clinical trials (NCT03945162) for the PDT-based intravesical treatment of non-muscle invasive bladder cancer using green light.[63] Based on these promising results, efforts are currently focused on the development of new metal-based PSs with operability at long wavelengths (500–800 nm) to achieve deep tissue penetration and treat large, hypoxic solid tumors.[67]

In this review, we present a detailed and comprehensive overview of the strategic design to develop innovative metal-based PSs by taking advantage of the unique photophysical and physicochemical properties of the coumarin scaffold. Our

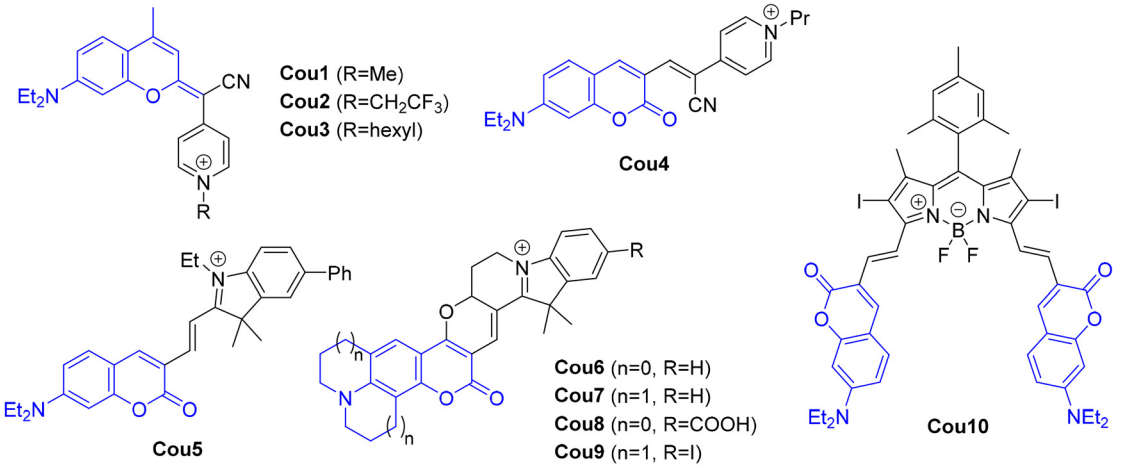

Fig. 4 Examples of coumarin-based PSs.

focus is on the structural diversity, photophysical and photochemical characteristics, and the phototherapeutic efficiency of PDT agents based on metal–coumarin derivatives. The review is systematically organized into two main sections based on the mode of integration of the coumarin into metal complexes:

1. Metal complexes where the coumarin fragment is attached to a ligand *via* a non-conjugated linker. This section explores systems where the coumarin is indirectly linked to the metal center.

2. Metal complexes where the coumarin is integrated into a ligand. This section examines cases where the coumarin plays a more direct role in coordination, either as a directly coordinated ligand or through conjugated linkers that enhance electronic communication between the coumarin and the metal center.

By categorizing the review in this manner, we aim to provide a clear and organized understanding of how coumarin integration influences the overall properties and efficacy of metal-based PDT agents. This structured approach allows for a more thorough comparison and analysis of the various strategies employed in the design of these advanced therapeutic agents. Particular emphasis is placed on metal–COUPY conjugates, where the metal complex is either a cyclometalated Ir(III) or Ru(II) complex. Additionally, we focus on Ru(II)–COUBPY complexes, in which the coumarin ligand is integrated into the coordination sphere of a Ru(II) polypyridyl complex *via* a bipyridine ligand.

II. Metal complexes where the coumarin fragment is attached to a ligand *via* a non-conjugated linker

a. PSs based on Ir(III)–COUPY conjugates

In 2019, Marchán, Ruiz, Brabec *et al.* described for the first time a cyclometalated Ir(III) complex conjugated to a COUPY coumarin[34] (**Ir–COUPY-1**, Fig. 5) as a new class of PSs that takes advantage of the photophysical properties of the organic fluorophore to enable activation at longer wavelengths compared to the metal complex alone. This PS exhibited promising PDT activity under both normoxic and hypoxic conditions upon visible light irradiation, the latter feature attributed to the photogeneration of type I superoxide ROS. The synthesis of the Ir(III)–COUPY conjugate involved forming an amide bond between the amino and carboxylic groups incorporated at key positions of the parent COUPY dye (**COUPY-a**) and the iridium complex (**Ir1**), respectively. **Ir–COUPY-1** was found to be water-soluble and highly stable in cell culture media.

The UV-Vis spectrum of **Ir–COUPY-1** was dominated by a strong absorption in the visible region of the electromagnetic spectrum due to the coumarin moiety, with a band centered around 550–565 nm depending on the solvent's polarity. The significant decrease in both the intensity and lifetime of the coumarin fluorescence in the conjugate indicated the existence of competitive excited-state processes. Conjugation of the metal complex to **COUPY-a** also resulted in a higher singlet oxygen quantum yield (Φ_Δ) in organic solvents compared to the coumarin alone upon irradiation with green light. However, none of the evaluated compounds exhibited singlet oxygen production in aqueous medium.

Thanks to the coumarin moiety, the cellular uptake of **Ir–COUPY-1** in living HeLa cells could be easily studied by confocal microscopy using yellow light excitation. This revealed accumulation in the cytoplasm, contrasting with the parent COUPY dye that accumulates in the mitochondria. The compound showed no cytotoxicity in the dark (IC_{50} > 200 μM) towards HeLa cells, whereas **COUPY-a** and **Ir1** displayed moderate cytotoxicity. However, under low doses of green (21 J cm^{-2}) or blue (28 J cm^{-2}) light, the IC_{50} values were 2.51 and 1.32 μM, yielding PI values of 85 and 161, respectively. The Ir(III)–COUPY conjugate maintained its high photocytotoxicity under hypoxic conditions (2% O_2), with a hypoxia index (HI) close to 1. This index, defined as the ratio of light IC_{50} in nor-

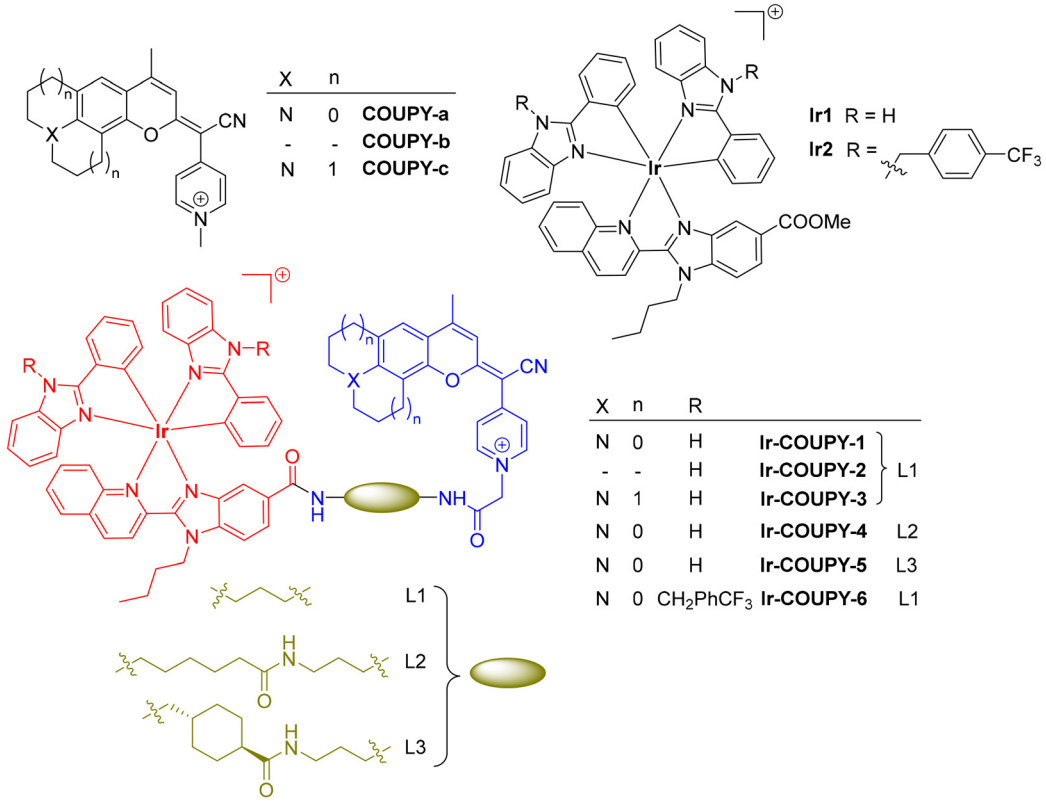

Fig. 5 Structures of Ir(III)–COUPY PSs based on the conjugation of COUPY dyes and cyclometalated Ir(III) complexes.

moxia to light IC_{50} in hypoxia, provides an idea of the potency of a given PS under hypoxia compared to normoxia (21% O_2). These results confirmed a strong phototoxic effect of the Ir(III)–COUPY PS even under challenging hypoxic conditions, compared with the non-conjugated parent compounds, particularly under green light irradiation.

ROS photogeneration studies in HeLa cells indicated that **Ir–COUPY-1** generated significantly more ROS than **Ir1** and **COUPY-a**. The use of various ROS scavengers confirmed that the primary ROS produced by **Ir–COUPY-1** was $^{\bullet}O_2^-$, making it a promising type I PS. This was a significant improvement over the iridium complex alone, which primarily produces singlet oxygen. The production of superoxide by **Ir–COUPY-1** was further confirmed in the absence of cells through spectroscopic methods using the DHR123 probe and electron paramagnetic resonance (EPR),[37] and correlated with cell death according to cellular viability experiments in the presence of the superoxide tiron scavenger. The ability of **Ir–COUPY-1** to function under hypoxia highlighted the potential of metal–COUPY conjugates as promising PS candidates for treating hypoxic tumors, which are resistant to traditional PDT that relies mainly on singlet oxygen photogeneration.

Ir–COUPY-1 also showed promising results for the PDT treatment of prostate cancer.[35] It was found to effectively eliminate both differentiated prostate cancer cells and prostate cancer stem cells (CSCs), which are often resistant to conventional therapies, making it significant for preventing cancer relapse and metastasis. The compound was able to penetrate the inner layers of 3D tumor spheroids, enhancing its therapeutic effect and showing high selectivity for tumor cells over noncancerous cells. **Ir–COUPY-1** was shown to induce apoptosis and autophagy, likely due to ROS generation under green light irradiation, contributing to its effectiveness. All these findings suggest that **Ir–COUPY-1** PS holds great potential to treat aggressive and resistant forms of prostate cancer.

Two subsequent studies focused on synthesizing a series of Ir(III)–COUPY conjugates (**Ir–COUPY-2–6**; Fig. 5) to explore structure–activity relationships (SARs).[37,38] The primary aim of the first study[37] was to assess how structural modifications within the COUPY scaffold influenced the photophysical, photochemical and photobiological properties of the resulting Ir(III)–COUPY PSs (**Ir–COUPY-2–5**). As shown in Fig. 5, the original cyclometalated Ir(III) complex **Ir1** was conjugated to three COUPY dyes using either flexible or rigid linkers. As expected, the absence of the *N*,*N*-diethylamino EDG at the 7-position of the coumarin moiety resulted in a significant blue-shift of the λ_{max} of **Ir–COUPY-2** (451 nm *vs.* 555 nm for **Ir–COUPY-1** in ACN). In contrast, the introduction of a julolidine-fused analogue caused a red-shift in both absorption and emission maxima (λ_{abs} = 580 nm and λ_{em} = 647 nm for **Ir–COUPY-3** in ACN) compared to the original **Ir–COUPY-1** (*ca.* 25 and 32 nm, respectively). Conjugates **Ir–COUPY-4** and **5** showed similar absorption and emission maxima in all investigated solvents compared to the original **Ir–COUPY-1**, since they contain the same coumarin.

The (photo)cytotoxicity studies revealed that all of the new Ir(III)–COUPY conjugates exhibited high phototoxicity under green light irradiation, except **Ir–COUPY-2**, while remaining non-toxic in the dark (IC_{50} > 250 μM).[37] The compounds effectively induced cell death in various cancer cell lines, including melanoma (A375, SK-MEL-28), ovarian cancer (A2780, A2780cis), and cervical cancer (HeLa), with significant sensitivity observed in cisplatin-resistant A2780cis cells, suggesting their potential to overcome drug resistance. The PI values varied among the cell lines, with the highest values in A2780cis cells (Table 1), and conjugates **1**, **4** and **5** demonstrated the best phototoxic profiles under green light irradiation. Despite showing a similar PI value, **Ir–COUPY-3** was considered a less effective PS since its photocytotoxic effect was very similar to that of the other conjugates, but required a higher intracellular accumulation to achieve comparable IC_{50} values, as inferred from cellular uptake studies by ICP-MS in A2780cis cells. Interestingly, the absence of the EDG at the 7-position in **Ir–COUPY-2** led to a loss of photocytotoxicity whereas the use of longer linkers, either flexible (**Ir–COUPY-4**) or rigid (**Ir–COUPY-5**) sharing the same coumarin moiety as **Ir–COUPY-1**, resulted in no significant changes in photocytotoxicity under normoxia. Under hypoxic conditions, the phototoxicity decreased but remained significant, with **Ir–COUPY-4** and **5** showing enhanced activity compared to the parent conjugate **Ir–COUPY-1**, with HI values close to 2 and PI values of >132 and >147, whereas **Ir–COUPY-1** exhibited a 5-fold decrease in cytotoxicity.

All conjugates were found to increase cellular ROS levels under green light irradiation, except for **Ir–COUPY-2**, which correlates with its lack of phototoxicity. In good agreement with the results from phototoxicity studies, ROS production under hypoxia was significantly higher for **Ir–COUPY-1**, **-4**, and **-5**. Furthermore, the photoinduced cell death mechanism was studied in A2780cis cells using the annexin V/propidium iodide (AV/PI) labeling method, which revealed that **Ir–COUPY-1**, **-3–5** induced necrosis. This mechanism of cell death can trigger inflammation and immune response, increasing toxicity in cisplatin-resistant tumors and highlighting their potential as PSs for PDT treatment.

The photoinduced anticancer activity of the Ir(III)–COUPY conjugates was also characterized against A2780cis MCTS. Consistent with the results of phototoxicity studies in 2D cellular models under hypoxic conditions, **Ir–COUPY-1**, **4** and **5** were able to inhibit the growth of A2780cis tumor spheres compared to conjugates **2** and **3**, which did not demonstrate significant tumor inhibition under the same experimental conditions.

After examining how modifications to both the coumarin and the linker influence the photobiological properties of the Ir(III)–COUPY conjugates, the subsequent step was to investigate the effects of modifying the parent iridium complex **Ir1**.[38] Interestingly, the incorporation of trifluorobenzyl groups in the cyclometalated ligands of the iridium complex (**Ir2**), enhanced the photophysical properties of the resulting conjugate (**Ir–COUPY-6**, Fig. 5), including higher absorptivity and luminescence quantum yield compared to **Ir–COUPY-1** and **-3**, which contain the same coumarin and linker.

In terms of biological activity, the **Ir–COUPY-6** conjugate demonstrated potent photocytotoxicity against A2780cis and breast cancer cells (EO771), efficiently generating type I and II ROS under red light irradiation (620 nm), leading to an enhanced PI under red light irradiation (>208) compared to green light (>134) in the cisplatin-resistant ovarian cancer cell line (Table 1). As previously stated, the use of red light is particularly advantageous as it penetrates deeper into tissues, making it more effective for treating large solid tumors. In contrast, similar PI values were obtained for **Ir–COUPY-1** and **-3** following red-light treatment compared to green light treatment, highlighting the key role of the trifluorobenzyl groups in the biological activity of the PS. Additionally, the **Ir–COUPY-6** conjugate showed a HI value close to 1 when evaluating photocytotoxicity under hypoxia in both EO711 and A2780cis cancer cells, indicating that its activity was not entirely dependent on

Table 1 (Photo)cytotoxicity of Ir(III)–COUPY conjugates, COUPY dyes and Ir(III) complexes towards A2780cis cells under green and red-light irradiation, both under normoxic (21% O_2) and hypoxic (2% O_2) conditions expressed as IC_{50} values (μM)[a]

	Dark		Green light			Red light		
Compound	Normoxia	Hypoxia	Normoxia	Hypoxia	PI[b] (N/H)	Normoxia	Hypoxia	PI[b] (N/H)
COUPY-a	>250	>250	2.1 ± 0.2	2.5 ± 0.2	>119/100	7.1 ± 0.4	5.9 ± 0.9	>35/>42.4
COUPY-b	>250	>250	>250	>250	—	—	—	—
COUPY-c	15 ± 2	34 ± 5	0.15 ± 0.04	0.6 ± 0.1	100/36.4	0.7 ± 0.1	0.37 ± 0.04	21.4/92
Ir1	>250	>250	1.5 ± 0.4	11 ± 2	>167/>22.7	4.5 ± 0.3	—	>56/—
Ir2	>250	>250	3.5 ± 0.4	—	>71/—	9 ± 2	—	>28/—
Ir-COUPY-1	>250	>250	0.70 ± 0.06	3.8 ± 0.3	>357/>65.8	0.71 ± 0.02	1.6 ± 0.2	>352/>156
Ir-COUPY-2	>250	>250	61 ± 8	31 ± 7	>4.1/>8.1	—	—	—
Ir-COUPY-3	>250	>250	1.04 ± 0.02	8 ± 1	>240/>31.3	1.2 ± 0.1	5 ± 1	>208/>50
Ir-COUPY-4	>250	>250	1.1 ± 0.2	1.9 ± 0.2	>227.3/>131.6	—	—	—
Ir-COUPY-5	>250	>250	0.93 ± 0.04	1.7 ± 0.3	>268.8/>147.1	—	—	—
Ir-COUPY-6	>250	>250	1.9 ± 0.3	—	>134	1.2 ± 0.2	1.4 ± 0.5	>208/>179

[a] Cells were treated for 2 h (1 h incubation and 1 h irradiation with green or red light at 520 nm or 620 nm, respectively) followed by 48 h of incubation in drug-free medium. Dark analogues were kept in the dark. Data expressed as mean ± SD from three independent experiments. [b] PI = phototherapeutic index defined as IC_{50} (dark-non-irradiated cells)/IC_{50} (irradiated cells).

high oxygen concentration. In contrast, **Ir–COUPY-1** and **-3** exhibited a 2-fold and 4-fold loss of photocytotoxicity under hypoxia, respectively.

Beyond $^{\bullet}O_2^-$ photogeneration, **Ir–COUPY-6** was also capable of producing hydroxyl radical ($OH^{\bullet}$) in hypoxia under red-light irradiation, as well as the photo-oxidation of NADH, an enzyme involved in mitochondrial electron transfer during cellular respiration. Furthermore, the type I PDT activity was theoretically supported by density functional theory (DFT) calculations, which demonstrated that the photoinduced electron transfer between the coumarin moiety and the Ir(III) complex favored superoxide formation. Further biological studies on the **Ir–COUPY-6** conjugate confirmed that it induced apoptosis under red light irradiation, suggesting that the cell death mechanism can be modulated by modifications to the Ir(III) complexes as well as by the wavelength of irradiation. Importantly, **Ir–COUPY-6** was found highly phototoxic against EO771 MCTSs under red-light irradiation and showed no signs of toxicity or adverse effects *in vivo*, as a 5 mg kg^{-1} dose was well tolerated by mice. Taken together, this study demonstrated that the conjugation between COUPY dyes and rationally designed Ir(III) complexes represents a frontier strategy for the development of new red light-activated PSs capable of operating under hypoxia.

b. PSs based on Ru(II)–COUPY conjugates

Based on the excellent performance of Ir(III)–COUPY conjugates under hypoxic conditions when irradiated with visible light, and the broad applications of ruthenium(II) polypyridyl complexes in cancer phototherapy, a **Ru–COUPY** conjugate (Fig. 6) was designed as a new metal–coumarin PS that could be activated with longer wavelengths.[36] As previously stated, far red and NIR light offers several advantages over short wavelengths, including deep tissue penetration due to its lower absorption and scattering by biological tissues. For this reason, a julolidine-fused CF_3-containing coumarin derivative with an increased push–pull effect (**COUPY-d**) was selected to be conjugated with a Ru(II) complex containing two dipyrido [3,2-*d*:20,30-*f*]quinoxaline (dpq) N^N ligands and a methyl 1-butyl-2-arylbenzimidazolecarboxylate ligand (**Ru1**). This compound was previously reported to exhibit high phototherapeutic potency under green light irradiation in hypoxic conditions.[68] The resulting Ru(II)–COUPY conjugate exhibited absorption and emission maxima in the far-red/NIR region of the electromagnetic spectrum (626 and 698 nm, respectively), which were red-shifted compared to the two separated components (*e.g.* λ_{max} = 561 nm and 615 nm for **COUPY-d** and **Ru1**, respectively). **Ru–COUPY** was able to generate singlet oxygen in ACN and DCM under green light irradiation, as well as superoxide in PBS, thereby reproducing a key feature of Ir (III)–COUPY conjugates.

Ru–COUPY showed no cytotoxicity in the dark (>300 μM) towards colon cancer cell lines (human HT-29 and murine CT-26), as well as cervix adenocarcinoma cells (HeLa), and minimal toxicity against A2780 ovarian cancer cells (IC_{50} = 97 ± 10 μM). In contrast, **COUPY-d** and **Ru1** exhibited moderate (35–44 μM) and high (0.8–7 μM) dark cytotoxicity, respectively. When irradiated with red light (620 nm), **Ru–COUPY** showed higher PI values than **Ru1**, but similar to **COUPY-d** in some cancer cell lines, notably achieving a PI >300 in CT-26 cells. A chromatic screening using different wavelength irradiation, ranging from red (620 nm) to NIR (740 nm and 770 nm), against HT-29 cells, revealed that **Ru–COUPY** maintained cell killing efficacy upon 740 nm irradiation in the same micromolar range as with other red-light treatments, with a PI > 42. By contrast, the phototherapeutic clinical drug PpIX did not show any NIR-photocytotoxicity up to 300 μM. Under hypoxia, **Ru–COUPY** exhibited PI values >23 and a HI of 1.8, indicating a significant enhancement in photobiological properties under hypoxic conditions when the coumarin was conjugated to ruthenium. **Ru–COUPY** also demonstrated the ability to produce singlet oxygen and superoxide in cells under normoxia, and to a lesser extent, under hypoxia.

Overall, the conjugation of a far-red/NIR emitting COUPY dye with a cyclometalated Ru(II) polypyridyl complex enabled the construction of a potent PS that addresses some of the key drawbacks of conventional metal-based PDT agents, such as dark cytotoxicity and inefficacy under hypoxia. **Ru–COUPY** exhibits other notable features, including water solubility, stability in biological media, and high photostability, along with luminescent properties that aid in bioimaging and phototherapy. Furthermore, this PS can effectively generate both type I superoxide and type II singlet oxygen under low doses of

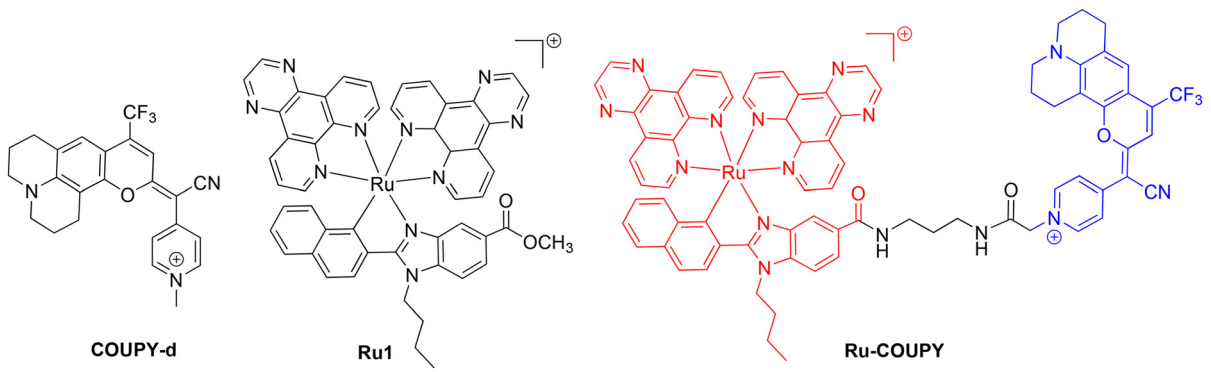

Fig. 6 Structure of Ru(II)–COUPY conjugate and of the parent coumarin and Ru(II) complex.

NIR light, even in hypoxic conditions, as confirmed by *in vitro* studies on HT-29 colon cancer cells, achieving high PI values. This conjugation approach offers a good opportunity to develop new NIR- and hypoxia-active Ru(II)-based theragnostic PSs using tunable, low molecular-weight COUPY fluorophores.

c. Other metal–coumarin PS

Zhu and co-workers developed NIR-activatable platinum(IV) complexes as potential photo-oxidant anticancer agents.[69] These complexes, derived from carboplatin (**Pt1**) and oxaliplatin (**Pt2**), feature a coumarin-based photosensitive ligand (Fig. 7) and exhibit stability in the dark while undergoing efficient reduction to Pt(II) drugs under two-photon irradiation at 880 nm. Their activation mechanism suggests a photoactivated chemotherapy (PACT) mechanism rather than a PDT mechanism. Biochemical studies confirmed that **Pt1** and **Pt2** could oxidize nucleic acids, proteins, and lipids even in oxygen-deprived environments. Upon irradiation, their cytotoxicity increased significantly (461-fold relative to that of the corresponding Pt(II) drugs), particularly against cancer stem cells, a key factor in metastasis and chemotherapy resistance. Unlike conventional Pt(IV) prodrugs, which primarily target DNA, these photo-oxidants accumulate in the endoplasmic reticulum (ER), triggering oxidative stress and immunogenic cell death (ICD). Further investigations into compound **Pt1** revealed that photoactivation led to glutathione and lipid oxidation, severe oxidative bursts, ER stress, and a decrease in intracellular pH. This dual mechanism resulted in rapid, non-classical necrosis and immune activation. *In vivo* studies demonstrated that intravenous administration of **Pt1**, followed by NIR irradiation, effectively inhibited tumor growth and metastasis while enhancing T lymphocyte infiltration in treated mice. These findings highlight the potential of Pt–coumarin-based photo-oxidants as promising candidates for targeted, oxygen-independent anticancer therapy.

III. Metal complexes in which the coumarin is incorporated into a ligand

a. Coumarin directly coordinated as a ligand

Due to their strong chromophoric properties, excellent electron-donating ability, and efficient light-harvesting capabilities, coumarins have garnered significant attention as versatile ligands in the development of metal-based PSs.[70] Coumarins can act as mono- or bi-dentate ligands, offering flexibility in coordinating with metal centers and enabling the design of complexes with diverse geometries and functionalities.[71] Furthermore, their ability to form stable metal complexes through oxygen or nitrogen donor atoms ensures structural robustness and long-term activity. As a result, a wide range of coumarin-containing metal complexes have been explored, including Pt(IV), Ir(III), Fe(III) and Co(II/III) compounds, which demonstrate the versatility and applicability of these ligands (Fig. 8–10).

Sadler and colleagues reported photoactivatable *trans*-diazidopyridine Pt(IV) complexes with different axial ligands: one containing a hydroxide ligand along with a coumarin ligand (**Pt3**, monofunctionalized) and another lacking the hydroxide ligand but featuring a second dichloroacetate (DCA) ligand (**Pt4**, difunctionalized).[72] These complexes were photoactivatable with blue light, generating Pt(II) species and releasing both axial ligands. The monofunctionalized complex **Pt3** exhibited greater photoselectivity towards A2780 cells due to its low cytotoxicity in the dark, whereas the difunctionalized complex **Pt4** showed selectivity towards A2780 cells both in the dark and under irradiation, with high cellular accumulation. Synchrotron techniques were employed to investigate the behavior of these prodrugs within cells and to visualize the localization of Pt after treatment with and without irradiation, as well as to observe changes in cellular morphology in PC3 cancer cells.[73] Post-irradiation, the **Pt3** compound was uniformly distributed within the cells, suggesting multiple cellu-

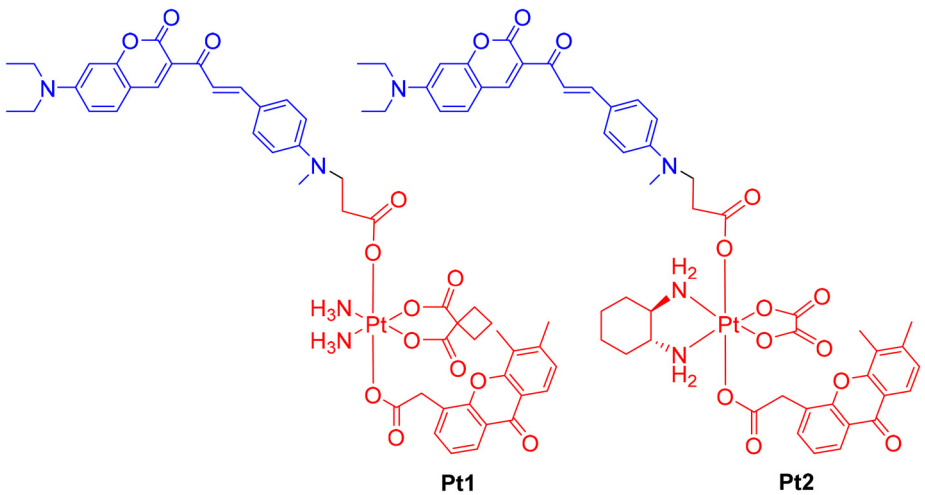

Fig. 7 NIR-activatable Pt(IV)–coumarin PSs.

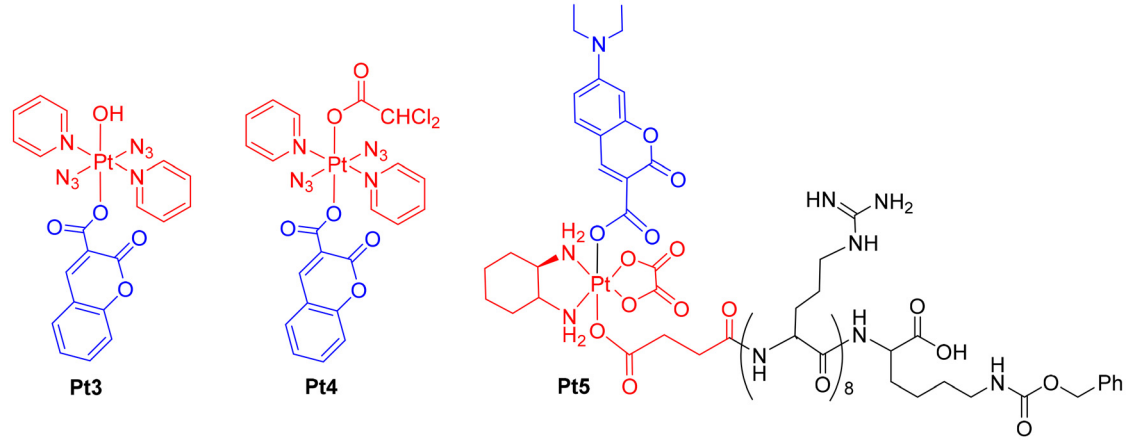

Fig. 8 Pt(IV)-based PSs with coumarin directly coordinated as a ligand.

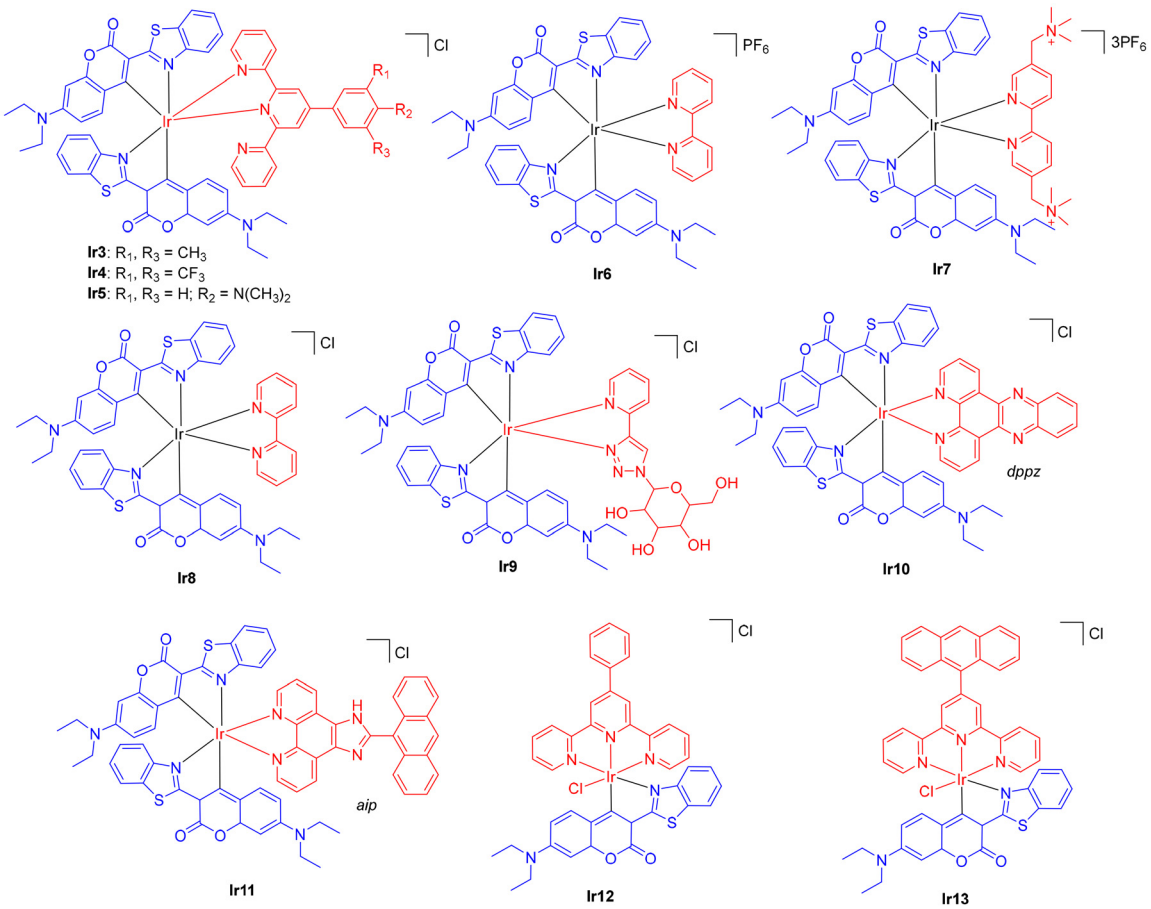

Fig. 9 Ir(III)-based PSs with coumarin C6 directly coordinated as C^N ligand.

lar targets and increased Pt levels. Additionally, the partial reduction of the Pt(IV) to Pt(II) after photoactivation implies that both Pt(IV) and Pt(II) species were involved in the mechanism of action. The formation of photolysis products near the cell membranes altered cellular morphology and suggested a radical-based mechanism of action.

In 2020, Zhu and co-workers developed a photocaged Pt(IV) conjugate, coumaplatin (**Pt5**), incorporating a coumarin and a cell-penetrating peptide. This complex remained stable in the dark and exhibited efficient photoactivation under physiological conditions.[74] After 1 hour of irradiation (450 nm, 8 mW cm^{-2}), HPLC analysis of A549cisR cell lysates detected the cou-

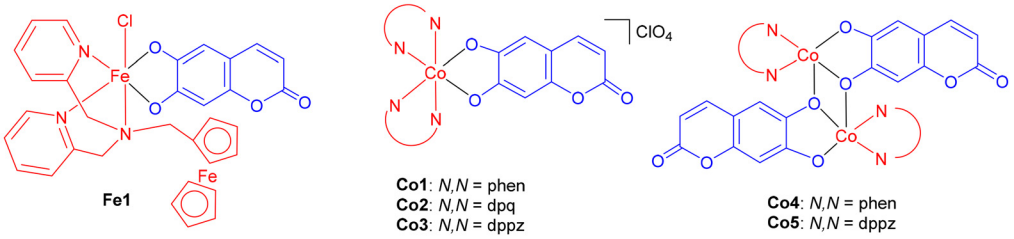

Fig. 10 Earth-abundant metal PSs with coumarin directly coordinated as O^O ligand.

marin ligand but not the Pt complex, indicating successful activation. Coumarin fluorescence was used to track the prodrug's activation and cellular localization. Upon activation, coumaplatin was effectively reduced to oxaliplatin, leading to an increased accumulation of Pt in genomic DNA. Notably, it displayed a unique activation pathway independent of p53 (E2F1-mediated) and strongly induced cellular senescence. Moreover, even at low concentrations, photoactivated coumaplatin significantly triggered ICD in resistant cells. This shift in oxaliplatin's subcellular distribution toward the nucleolus dramatically altered its mechanism of action, offering a novel strategy to overcome drug resistance.

Ir(III)-based PSs are particularly notable for their ability to generate intracellular ROS and act as photo-catalysts for the oxidation of endogenous nicotinamide adenine dinucleotide (NADH).[75] NADH plays a crucial role in cellular metabolism, including glycolysis and the tricarboxylic acid cycle, and is a key electron source in the mitochondrial electron transport chain. Depletion of NAD(P)H by photoactive Ir(III) complexes in cancer cells may help combat tumor hypoxia-related drug resistance. Huang *et al.* reported Ir(III) complexes containing coumarin C6, a coumarin derivative containing a benzothiazolyl group at position 3, as cyclometalated (C^N) ligands (**Ir3–5**) (Fig. 9).[76] Upon 525 nm green light irradiation, these complexes oxidized intracellular NAD(P)H with high turnover frequency (TOF; 1200 h^{-1}) and generated hydrogen peroxide and singlet oxygen *via* type I and type II pathways. The complexes exhibited remarkable necro-apoptotic anticancer activities, attributed to the synergistic effects of NAD(P)H photo-oxidation and ROS generation. Notably, **Ir4** showed a very high phototoxicity index (PI = 793), significantly higher than the clinically used photosensitizer 5-aminolevulinic acid (5-ALA, PI > 30) against HeLa cell monolayers. Additionally, **Ir4** demonstrated significant photo-catalytic anticancer effects in tumor-bearing mice. To enhance water solubility, Huang *et al.* also reported Ir(III)–coumarin complexes (**Ir6–Ir7**) featuring the same C^N coumarin 6-based ligand, along with 4,4′-bis(*N*,*N*,*N*-trimethylmethanaminium)-2,2′-bipyridine as the N^N ligand.[77] The water-soluble complex **Ir7** was highly potent as a photocatalyst for the oxidation of NAD(P)H and amino acids *via* a single electron transfer (SET) pathway. Under blue light irradiation (465 nm, 11.7 J cm^{-2}), **Ir7** induced remarkable photocytotoxicity against several cancer cell lines while remaining non-toxic to normal cells (PI: 40–172). In addition, the complex showed high *in vivo* photocatalytic anticancer efficiency, in both zebrafish and mice tumor models, where tumor growth was significantly retarded after light irradiation. Continuing their research, Sadler *et al.* prepared glucose-bound Ir(III)–coumarin derivatives that showed increased water solubility and biocompatibility.[78] The non-glycosylated **Ir8** was used as control. The glucose derivatives were efficient in generating ROS and photo-oxidizing NAD(P)H under blue light with turnover number (TON) and TOF values four times higher than those observed in previously described Ir(III) complexes. In addition, **Ir9** showed a high PI (334) in HeLa cells after irradiation (465 nm, 11.7 J cm^{-2}). The **Ir9** complex was highly biocompatible as demonstrated by *in vivo* studies with zebrafish.

Banerjee *et al.* have successfully synthesized and characterized two new Ir(III)-based photocatalysts containing coumarin C6 as C^N ligands, **Ir10** and **Ir11**.[79] The anticancer potential of these complexes under light exposure was enhanced by extending the conjugation within the ligand framework (*e.g.*, dipyrido[3,2-*a*:2,3-*c*]phenazine (dppz) *vs.* 2-(anthracen-9-yl)-1*H*-imidazo[4,5-*f*][1,10]phenanthroline (aip)). The absorption spectra of **Ir10** and **Ir11** displayed a sharp coumarin-based band in the 450–550 nm range, along with a metal-to-ligand charge transfer (MLCT) band between 400–450 nm. These spectral features enabled green light-driven catalytic NADH oxidation and visible light-induced anticancer activity. Among the two, **Ir11** exhibited superior photocatalytic efficiency for NADH oxidation in aqueous solution, achieving a TON of approximately 66 and a TOF of around 1000 h^{-1}, whereas **Ir10** showed a TON of about 28 and a TOF of 841 h^{-1}. This suggests that the extended conjugation in **Ir11** enhances its electron-accepting properties compared to **Ir10**. Both complexes demonstrated strong photo-cytotoxicity against cancer cells under both normoxic and hypoxic conditions, with high PI values ranging from >28 to 71. The slightly greater phototoxicity of **Ir11** compared to **Ir10** could be attributed to its increased conjugation, which may improve lipophilicity, cellular uptake, and photosensitivity. The apoptotic anticancer activity of these complexes under light exposure in normoxia was primarily driven by their ability to generate ROS and oxidize NADH within cells, thereby activating caspase 3. While many photocatalysts for cancer therapy under normoxia have been shown to exert their effects through a combination of NADH oxidation and $^1O_2$ production, **Ir10** and **Ir11** exhibited

an additional mechanism by generating hydroxyl radicals alongside $^1O_2$ and NADH oxidation.

Similarly, the recently developed Ir(III)–coumarin complexes, **Ir12** and **Ir13**,[80] have demonstrated promising photocatalytic and anticancer properties under green light irradiation (525 nm, 50.2 J cm^{-2}). Structurally, these complexes also incorporate coumarin C6 as C^N ligand, combined with either a phenyl-terpyridine (Ph-tpy) or anthracenyl-terpyridine (An-tpy) moiety, which modulates their photophysical and biological behavior. **Ir12** and **Ir13** efficiently catalyzed NADH oxidation in phosphate-buffered saline, exhibiting TOF values comparable to **Ir10** and **Ir11**, ranging from 840 to 1100 h^{-1}. Their ability to generate ROS, including $^1O_2$ and $^{\bullet}OH$, was attributed to a synergistic interplay of type I and type II photoreactions. Notably, **Ir13**, featuring the anthracenyl-terpyridine unit, displayed superior phototoxicity against MCF-7 and HeLa cancer cells while maintaining minimal dark cytotoxicity toward HEK-293 non-cancerous cells. The selectivity index (SI) for **Ir12** and **Ir13** reached up to 22, underscoring their potential as selective photosensitizers for PDT. Mechanistic investigations revealed that the anticancer activity of **Ir13** upon light activation was mediated by enhanced mitochondrial ROS accumulation, mitochondrial membrane depolarization, and caspase 3/7-driven apoptosis.

In addition, Banerjee *et al.* also explored the development and evaluation of a novel Fe(III) complex, [Fe(L)(esc)Cl] (**Fe1**),[81] with a ferrocene conjugated *N*,*N*,*N*-donor tridentate dipicolylamine ligand (ferrocenyl-*N*,*N*-bis((pyridin-2-yl)methyl)methanamine, L) and incorporating esculetin (6,7-dihydroxycoumarin), a naturally occurring coumarin catecholate derivative with anticancer and photosensitizing properties (Fig. 10). **Fe1** exhibited a ligand-to-metal charge transfer (LMCT) absorption band in the red region, enabling red light photo-toxicity in cancer cells. While non-toxic in the dark, the complex became highly toxic to cancer cells (HeLa, MCF-7, HaCaT) upon irradiation with visible light. Interestingly, **Fe1** exhibited phototoxicity even when was irradiated with a low dose of red light (600–720 nm, 50 J cm^{-2}), showing PI >3–6. The iron complex generated ROS and induced apoptotic cell death through photoredox and type II mechanisms. Notably, the dark toxicity of esculetin decreased upon complexation with Fe(III), and the complex remained non-toxic to normal cells (MCF-10A) even after light irradiation. This study highlights the tumor selectivity, bio-imaging capabilities, and mitochondria-targeted red light cytotoxicity of the Fe(III) complex, demonstrating the potential of coumarin-based PSs for cancer treatment. Moreover, the use of earth-abundant Fe offers a cost-effective and sustainable alternative to precious metals.

Co(III) complexes, with their rich photophysical and photochemical properties, as well as their low-energy absorption bands, are potential photocytotoxic agents. Hussain *et al.* have described heteroleptic Co(III) complexes with mixed ligands: phenanthroline-type based and a naturally derived coumarin compound, esculetin, with the stoichiometry [Co(B)$_2$(L)]ClO$_4$ (**Co1–3**) (Fig. 10).[82] Here, B represents an N,N ligand (1,10-phenanthroline, phen, dipyrido[3,2-*d*:2,3-*f*]quinoxaline, dpq, and dipyrido[3,2-*a*:2,3-*c*]phenazine, dppz), and L is the dianionic O,O-donor ligand esculetin. **Co1–Co3** exhibited significant toxicity in the presence of low-energy visible light (10 J cm^{-2}) and negligible toxicity in the dark against HeLa cells (PI >2–31). Notably, the dppz derivative (**Co3**) was the most active, followed by the dpq (**Co2**) and phen (**Co1**) compounds. The photocytotoxic activity correlated well with their lipophilicity. The **Co3** complex preferentially accumulates in the mitochondria of HeLa cells, as revealed by confocal microscopy studies. Additionally, it induces cell death *via* apoptosis through the generation of ROS *via* type I mechanism that generates hydroxyl radicals and efficiently induces visible light-mediated DNA cleavage. Furthermore, the **Co3** complex serves as a cellular imaging agent.

Very recently, Hussain *et al.* have also described a series of dinuclear Co(II) complexes (**Co4–5**)[83] with light-enhanced anticancer and antibacterial properties. In these complexes, phen and dppz acted as neutral N,N-donor ligands, while esculetin served as O,O-donor ligand. The **Co4** and **Co5** complexes displayed an absorption band within the 600–850 nm range, which can be attributed to a charge transfer transition. These electrically neutral compounds exhibited good stability in solution under both dark and irradiated conditions. Among them, the dppz-complex **Co5** demonstrated significant cytotoxicity against A549 lung carcinoma cells, with their potency markedly enhanced after a short (5-minute) exposure to deep-red (660 nm) and NIR (808 nm) laser light, achieving IC_{50} values in the range of ~8.9 to 14.9 μM. Importantly, they showed minimal toxicity toward normal NIH-3T3 fibroblast cells. Cellular studies indicated that the observed cell death was primarily driven by apoptosis resulting from mitochondrial damage. The enhanced anticancer activity was linked to the production of $^1O_2$ with a singlet oxygen quantum yield (Φ_Δ) of 0.13 for **Co5** upon exposure to red or NIR light, yielding stronger effects than 660 nm.

b. Coumarin attached to a ligand *via* a conjugated linker

In addition to using coumarin as a ligand itself, another strategy reported in the literature involves anchoring the coumarin moiety to a ligand *via* a π-conjugated linker.[70,84] This approach offers greater structural flexibility and can optimize orbital interactions, facilitating more efficient charge transfer and better control over the complex's photophysical properties.[85] In recent years, this strategy has been successfully applied to the development of various metal–coumarin complexes, particularly in the design of Ru(II)–coumarin PSs for PDT applications.

Although most Ru-based PSs reported in the literature contain N^N ligands,[86–88] the use of C^N ligands offers a significant advantage for developing type I PSs. The electron-donating nature of C^N ligands can elevate the energy level of the dπ(Ru) orbital, leading to a cathodic shift in the oxidation potential.[89,90] This shift facilitates electron transfer processes, providing a promising pathway for the generation of new type I PSs. In this context, Huang and co-workers designed type I PSs based on cyclometalated Ru(II) complexes incorporating a cou-

marin moiety into a cyclometalated ligand (2-(3,4-difluorophenyl)pyridine) *via* a carbon–carbon double bond (**Ru2**) (Fig. 11).[91] This complex demonstrated a lower oxidation potential and enhanced absorption in the visible region compared to its coumarin-free counterpart. PDT efficacy was assessed under both normoxic and hypoxic conditions using white light for 10 min. The results indicated that **Ru2** exhibited superior therapeutic performance *in vitro* (3.1% of cell viability at 20 μM) compared to the complex lacking the coumarin. Notably, even under hypoxia, **Ru2** maintained a strong PDT effect, likely due to direct charge transfer between the excited PS and a nearby substrate *via* a type I photochemical mechanism, generating highly oxidative hydroxyl radicals that contribute to tumor cell damage. Furthermore, studies in tumor-bearing mice confirmed the antitumor efficacy of **Ru2**, showing significant inhibition of tumor growth upon PDT treatment.

Nomula *et al.* reported two coumarin-based Ru(II)-polyimine complexes (**Ru3** and **Ru4**) which exhibit strong visible light absorption and possess long-lived triplet excited states (~12–15 μs) (Fig. 11).[92] The complexes were investigated for their interactions with DNA. The findings indicate that both **Ru3** and **Ru4** bind to calf thymus DNA (CT-DNA) through an intercalative mode, with binding constants (K_b) of 6.47×10^4 M^{-1} and 5.94×10^4 M^{-1}, respectively. DNA cleavage activity under visible light irradiation (450 nm) was examined by treating supercoiled pUC19 DNA with these complexes, resulting in the production of $^1O_2$ with $\Phi_\Delta = 0.67$ for **Ru3** and 0.42 for **Ru4**. Both **Ru3** and **Ru4** demonstrated efficient DNA cleavage, converting supercoiled DNA to nicked circular form at concentrations as low as 20 μM within 30 minutes of light exposure. Under the same conditions, **Ru3** produced a significant amount of linear DNA. The cytotoxicity of the complexes toward HeLa, BEL-7402, and MG-63 cells was evaluated using the MTT assay, and cellular uptake was observed in BEL-7402 cells *via* fluorescence microscopy. The complexes exhibited moderate cytotoxic effects, with IC_{50} values of 15.5, 19 and 20.0 μM for **Ru3**, and 19.8, 24.0, and 21.2 μM for **Ru4** towards HeLa, BEL-7402 and MG-63 cell lines, respectively.

Recently, Marchán, Gasser *et al.* described a family of potent PSs based on Ru(II) polypyridyl complexes incorporating 2,2′-bipyridyl ligands derived from COUPY coumarins, termed COUBPYs.[39] Ru–COUBPY complexes (**SCV42**, **SCV45**, and **SCV49**; Fig. 12) exhibit exceptional *in vitro* cytotoxicity against colon cancer cells (CT-26) upon irradiation with light within the phototherapeutic window, under both normoxic and hypoxic conditions, while remaining non-toxic in the dark.

The photophysical properties of Ru–COUBPY complexes are strongly influenced by the coumarin ligand since they display absorption bands beyond 500 nm, which are absent in the complex lacking the coumarin moiety ($[Ru(bpy)_3]^{2+}$). Computational studies confirmed that these bands involve a contribution from COUPBY ligands. For **SCV42** and **SCV45**, two sharp yet almost-fused bands are observed in the 500–600 nm range, while **SCV49** exhibits a broader band around 570 nm, with some weak absorption extending beyond 700 nm. These spectral characteristics allowed the compounds to be photoactivated with visible light, ranging from green (540 nm) to far-red (670 nm) light, and even with NIR light (740 nm). Additionally, Ru–COUBPY complexes efficiently photogenerated type I (superoxide and hydroxyl radical) and type II (singlet oxygen) ROS, as assessed by spectroscopic methods using fluorogenic probes and EPR. Among the series, **SCV42** exhibited the highest singlet oxygen production, although **SCV49** was capable of generating ROS even under

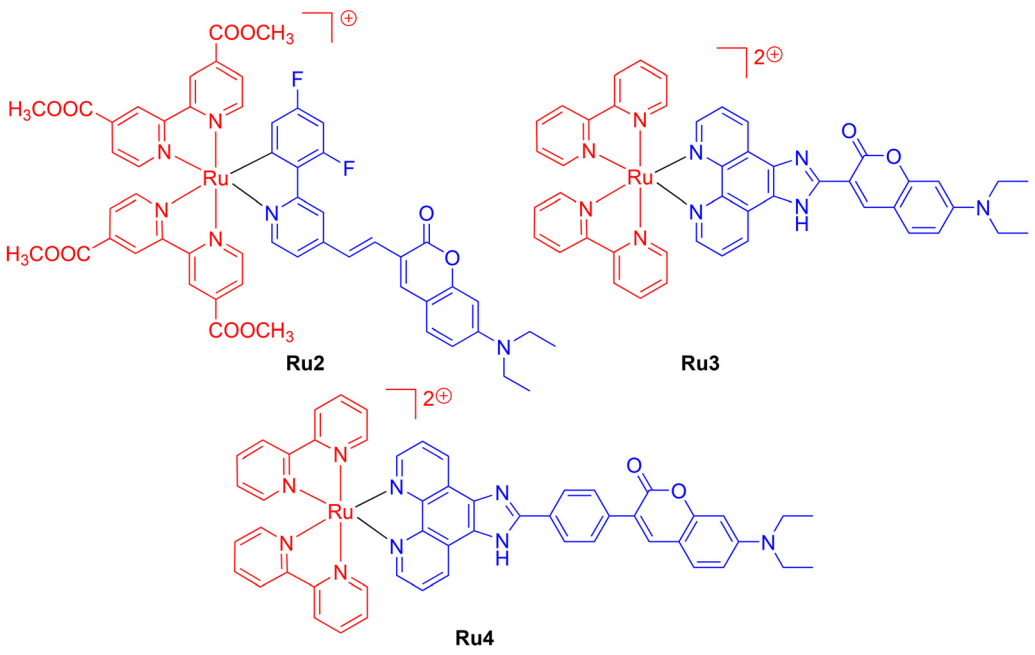

Fig. 11 Ru(II)-based PSs with coumarin attached to a ligand *via* a π-conjugated linker.

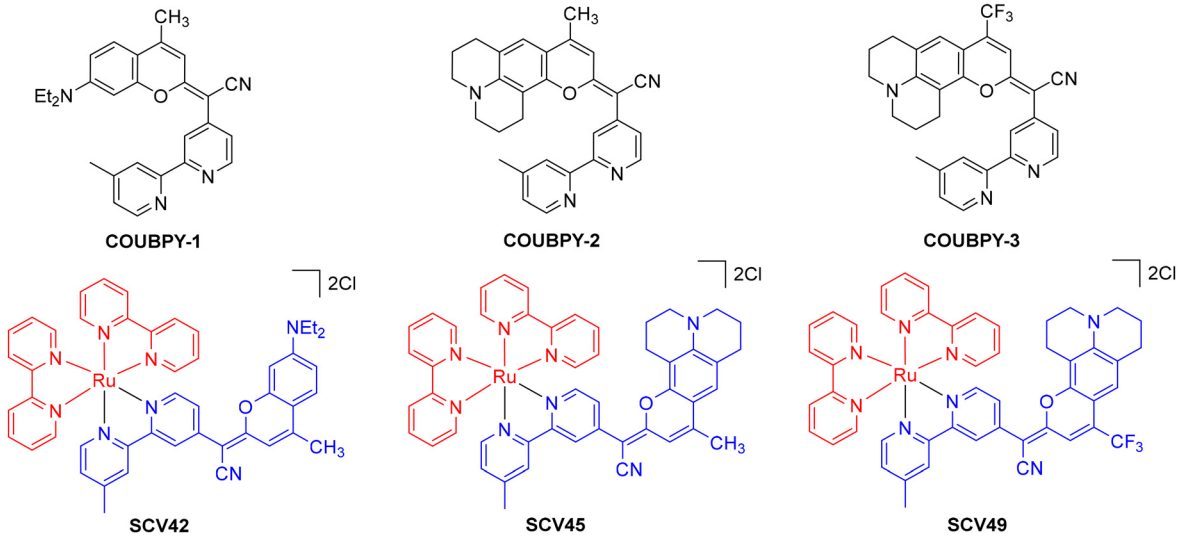

Fig. 12 Structure of COUBPY ligands and of Ru–COUBPY complexes.

red-light irradiation. **SCV45** appeared to be the least photostable in culture media, indicating the negative effect of the julolidine group, while the incorporation of a trifluoromethyl group in the coumarin led to increased photostability. Moreover, the compounds displayed good water solubility and high dark and light stability in complete cell culture medium.

Cellular uptake studies using confocal microscopy confirmed that **SCV42** and **SCV45** primarily localized in the mitochondria, whereas **SCV49** also accumulated in lysosomes and lipid droplets. Ru–COUBPY complexes exhibited no cytotoxicity in the dark (>250 μM) towards CT-26 cells, but after irradiation with green, deep-red and far-red light, the IC_{50} values of all three complexes were in the nanomolar range, leading to exceptional high PI values of >30 000 in some cases. As shown in Table 2, the best results were obtained for complex **SCV42** under green light irradiation (IC_{50} = 8.2 nM, PI >30 487) and for **SCV49** under deep-red light (IC_{50} = 7.4 nM, PI >33 783). Remarkably, **SCV49** maintained high photocytotoxicity in the submicromolar range even under irradiation at 740 nm, with a PI >329.

Under hypoxic conditions, **SCV42** and **SCV49** retained high nanomolar cytotoxicity under visible light irradiation (Table 2). Once more, **SCV42** performed best under green light (IC_{50} = 35 nM), while **SCV49** exhibited excellent phototoxicity under green, deep-red and far-red light (*e.g.* IC_{50} = 74 nM at 670 nm), and maintained micromolar activity upon NIR light. The strong phototoxic activity of Ru–COUBPY PSs under hypoxia was attributed to their ability to simultaneously photogenerate type I and type II ROS.

Finally, the *in vivo* safety and efficacy studies in mice highlighted the potential of Ru–COUBPY PSs for PDT cancer treatment, especially the lead compound **SCV49**. This Ru–COUBPY complex demonstrated a favorable *in vivo* pharmacokinetic profile and excellent toxicological tolerability in healthy mice following intraperitoneal administration. This was evidenced by various parameters such as body weight, food consumption, organ weight, and comprehensive hematological and biochemical analyses. Additionally, the remarkable *in vitro* phototoxicity of **SCV49** was confirmed in an animal model, showing potent tumor inhibition in mice bearing subcutaneous CT-26

Table 2 (Photo)cytotoxicity of Ru–COUBPY complexes **SCV42** and **SCV49** towards CT-26 cancer cells under visible and NIR light irradiation, both under normoxic (21% O_2) and hypoxic (2% O_2) conditions expressed as IC_{50} values (μM)[a]

	SCV42				**SCV49**			
	Normoxia		Hypoxia		Normoxia		Hypoxia	
	IC_{50} (μM)	PI[b]	IC_{50} (μM)	PI[b]	IC_{50} (μM)	PI[b]	IC_{50} (μM)	PI[b]
Dark	>250	—	>250	—	>250	—	>250	—
540 nm	0.0082 ± 0.0006	>30 487	0.035 ± 0.005	>7143	0.025 ± 0.002	>10 000	0.086 ± 0.011	>2907
645 nm	0.048 ± 0.003	>5208	0.920 ± 0.09	>272	0.0074 ± 0.0006	>33 783	0.076 ± 0.008	>3290
670 nm	1.460 ± 0.450	>171	13.24 ± 3.64	>19	0.036 ± 0.003	>6944	0.074 ± 0.005	>3378
740 nm	31.3 ± 6.1	>8	>100	—	0.76 ± 0.06	>329	9.56 ± 2.15	>26

[a] Cells were incubated for 4 h at 37 °C, followed by either 1 h in the dark or irradiation under the specified light conditions. Cell viability was determined after 44 h using the resazurin assay. [b] PI = phototherapeutic index defined as IC_{50} (dark-non-irradiated cells)/IC_{50} (irradiated cells).

tumors upon intratumoral administration under deep-red light irradiation (660 nm).

IV. Overall structure–activity relationships of metal–coumarin complexes

To offer a broader perspective on the therapeutic relevance of metal–coumarin PSs, we present a comparative analysis of the complexes across different metal centers (Ir(III), Ru(II), Pt(IV), Fe(III) and Co(III)), coumarin integration strategies, and phototherapeutic conditions (Table S1, ESI†). The table compiles relevant data, including absorption maxima (λ_{abs}), molar extinction coefficients (ε), singlet oxygen quantum yields (Φ_Δ), light conditions used for photocytotoxicity studies, and biological activity under normoxic and hypoxic conditions.

The analysis reveals several key trends:

1. *Metal center influence*:

Among the different metal centers, Ir(III) and Ru(II) complexes consistently exhibit superior performance, especially in hypoxic environments, owing to their strong spin–orbit coupling that promotes ISC and triplet-state formation. These long-lived excited states facilitate both type I and type II ROS generation. Notably, cyclometalated Ir(III)– and Ru(II)–COUPY conjugates achieved high phototoxicity indices (PI >100–200 in multiple cases) and potent activity in drug-resistant cancer cell lines, even under hypoxia, which was attributed to efficient type I ROS production due to intramolecular photoinduced electron transfer between the coumarin moiety and the metal complex. This activity was greatly surpassed when coumarin ligands were integrated into the coordination sphere of Ru(II) polypyridyl complexes, allowing Ru(II)–COUBPY complexes to achieve PI values greater than 30 000 upon irradiation with light within the phototherapeutic window. While less potent, Fe(III) and Co(III) complexes demonstrated promising selectivity, mitochondrial targeting, and compatibility with red or NIR light. Their earth-abundant nature and sustainable profiles make them appealing candidates for further development despite lower quantum yields or extinction coefficients. Pt(IV) complexes showed potential for oxygen-independent activation, likely *via* photoreduction pathways that bypass ROS altogether.

2. *Coumarin integration strategy*:

The mode of coumarin incorporation significantly affects the compound's behavior.

(i) Non-conjugated coumarin linkers: In metal–COUPY systems, the coumarin is appended *via* flexible linkers to the metal complex. These structures exhibit efficient cellular uptake, tunable luminescence, and excellent selectivity. Although singlet oxygen quantum yields are typically low (Φ_Δ < 0.01), the biological response is pronounced through type I ROS generation, particularly under dual green/red light irradiation.

(ii) Direct integration into the coordination sphere: complexes in which coumarin functions as a chelating ligand or part of a π-conjugated system often display enhanced metal-to-ligand charge transfer (MLCT) characteristics, higher molar extinction coefficients, and improved ROS photogeneration. For instance, **Ir7–Ir9** and Ru–COUBPY complexes show robust activity with singlet oxygen and/or superoxide and hydroxyl radical production.

3. *Ligand design and absorption properties*:

Another key determinant of PDT efficacy is the spectral profile. Complexes with strong absorption in the 500–650 nm region align well with the phototherapeutic window, offering deeper tissue penetration. π-Extended ligands (*e.g.*, anthracenyl- or phenyl-terpyridines, dppz) not only red-shift the absorption maxima but also boost light-harvesting capability and enhance intersystem crossing rates.

4. *Photobiological performance across cell lines and oxygen conditions*:

A consistent observation across the dataset is the superior performance of metal–coumarin PSs in drug-resistant cell lines (*e.g.*, A2780cisR, A549R) and under hypoxia, conditions typically challenging for classical PDT. Phototoxicity indices exceeding 300 in these settings reflect the critical importance of designing PSs capable of functioning *via* oxygen-independent or mixed ROS-generation pathways.

V. Conclusions and outlook

PDT is a clinically approved technique for treating various medical conditions. It uses a light-activated drug, known as a photosensitiser, and molecular oxygen. Transition metal complexes with photofunctional properties are highly valued as PSs due to their versatile photophysical and photochemical characteristics. These features make them suitable drug candidates for bioimaging and therapeutic applications, including anticancer PDT. This review highlights the pivotal role of coumarin derivatives, known for their exceptional (photo)chemical versatility, in improving the photophysical, photochemical and photobiological properties of metal-based PSs. The discussion primarily focuses on cancer phototherapy and is systematically categorized into two major sections based on the integration approach of the coumarin within the metal complexes.

For metal complexes where the coumarin is attached to the metal core *via* non-conjugated linkers, particular emphasis was placed on metal–COUPY conjugates. These included cyclometalated Ir(III) and Ru(II) polypyridyl complexes linked to far-red/NIR-emitting coumarin-based COUPY fluorophores. Notably, the **Ir-COUPY-1** PS demonstrated activation with visible light, efficient cellular uptake in HeLa cells, and promising photocytotoxicity under both normoxic and hypoxic conditions upon irradiation with green and red light, attributed to the generation of superoxide type I ROS. Further studies on a series of Ir(III)–COUPY conjugates (**Ir–COUPY-2–6**) revealed structure–activity relationships, with specific modifications in the coumarin, spacer and ligand's metal complex enhancing

photocytotoxicity against resistant cancer cell lines. Similarly, the **Ru–COUPY** conjugate exhibited efficient activation by far-red and NIR light and improved photostability, proving effective under challenging hypoxic conditions. In parallel, Pt(IV)–coumarin complexes have also demonstrated potential for oxygen-independent chemotherapy, offering promising solutions to combat drug resistance.

The approach of integrating coumarin into ligands of the metal complex has also been widely explored in the literature. Among the examples where the coumarin is directly bound to the metal coordination sphere, coumarin C6 containing a benzothiazolyl group at position 3 stands out. Ir(III)–coumarin complexes incorporating this coumarin as a C^N ligand along with different N^N co-ligands showed exceptional photocatalytic and anticancer properties under green light irradiation. Their synergistic type I and type II photoreactions facilitated ROS generation and NAD(P)H photo-oxidation, mitochondrial ROS accumulation, membrane depolarization, and caspase 3-driven apoptosis.

Additionally, iron complexes like [Fe(L)(esc)Cl] (**Fe1**) with the natural coumarin derivative esculetin exhibited effective ROS generation and apoptosis induction through photoredox and type II mechanisms. These complexes combine tumor selectivity, mitochondrial targeting, and sustainability, leveraging the earth-abundant nature of iron as a cost-effective alternative to precious metals. Heteroleptic Co(III) complexes (**Co1–3**), composed of phenanthroline-based and esculetin ligands, displayed significant light-induced toxicity *via* type I ROS production and DNA cleavage, with negligible toxicity in the dark. These complexes also serve as cellular imaging agents and efficient PDT tools. Similarly, dinuclear Co(II) complexes (**Co4–5**) demonstrated enhanced anticancer and antibacterial efficacy under red or NIR light, inducing apoptosis primarily through mitochondrial damage.

The use of π-conjugated linkers instead of coumarin as direct ligands, provides structural flexibility and optimizes orbital interactions, significantly improving photophysical and photobiological properties. Coumarin's adaptability has driven the development of advanced metal-based PDT agents for diverse cancer treatments. Notably, type I PSs based on cyclometalated Ru(II) complexes, such as **Ru3** and **Ru4**, leverage C^N ligands like 2-(3,4-difluorophenyl)pyridine for strong visible light absorption, long-lived triplet excited states, and effective DNA interactions, establishing them as promising tools for phototherapeutic applications.

Ru–COUBPY PSs, where the coumarin scaffold is incorporated into the metal coordination sphere of Ru(II) polypyridyl complexes *via* a bipyridine ligand, have shown remarkable *in vitro* cytotoxicity against colon cancer cells when irradiated with light within the phototherapeutic window, under both normoxic and hypoxic conditions. This is due to their ability to generate type I and type II ROS. Notably, Ru–COUBPY complexes achieved exceptionally high PI values, exceeding 30 000 in certain cases upon irradiation with deep-red light. Furthermore, the Ru–COUBPY complex **SCV49** exhibited a favorable *in vivo* pharmacokinetic profile and excellent toxicological tolerability in healthy mice. This PS also exhibited potent tumor inhibition in mice bearing subcutaneous colorectal tumors under deep-red light irradiation (660 nm), underscoring the promising future of metal–coumarin PSs in advancing cancer treatment through PDT.

The development of metal–coumarin derivatives as innovative PSs has significantly advanced cancer phototherapy by improving light absorption in the phototherapeutic window, ROS photogeneration, and phototoxicity under both normoxic and hypoxic conditions. The promising results of the *in vivo* safety and efficacy studies with Ru–COUBPY complex **SCV49** highlight the translational potential of this new class of PSs. However, further comprehensive studies in animal models are needed to validate the efficacy of metal–coumarin PSs in clinically-relevant environments.

Future research should focus on rational ligand design to fine-tune photophysical properties, improve triplet-state lifetimes, and increase selectivity toward cancer cells. Expanding the scope of earth-abundant metal-based PSs also offers a sustainable and cost-effective alternative to noble metal systems. Synthetic scalability and stability of metal–coumarin complexes are critical aspects that also need to be addressed for clinical development. Another important aspect that needs attention is the lack of studies on the photoproducts generated from metal-based PSs, which may potentially cause undesired toxicity. Understanding the nature and effects of these photoproducts is crucial for developing safer and more effective PDT treatments. Another key challenge remains in enhancing tumor selectivity and bioavailability, which could be addressed through targeted drug delivery strategies based on conjugates with tumor-targeting moieties (*e.g.* peptides, antibodies and carbohydrates) that exploit receptors overexpressed on cancer cells, as well as nanoparticle formulations designed to accumulate in tumors.

For metal–coumarin complexes to be approved for use as drugs in humans, they must comply with the requirements set by regulatory agencies like the FDA and EMA. This involves detailed chemistry, manufacturing, and controls (CMC) documentation for investigational new drug (IND) submissions, ensuring the quality, safety, and efficacy of the products throughout their development and commercialization. Preclinical regulatory studies in animals must provide comprehensive data on dosing, toxicity and biodistribution. All these studies are essential to evaluate the potential risks of PS drug candidates before entering clinical trials.

Finally, advancements in light-delivery technologies, including upconversion nanoparticles and fiber-optic-guided illumination, may further expand PDT's applicability by enabling deeper tissue penetration and access to tumors located in challenging areas such as the throat, lung, and gastrointestinal tract. By addressing all these challenges through interdisciplinary efforts, metal–coumarin-based PSs have the potential to revolutionize PDT, offering more selective, efficient, and minimally invasive treatment options for cancer therapy. Additionally, integrating multimodal approaches, such as combining PDT with other modalities like photother-

mal therapy (PTT), sonodynamic therapy (SDT) or chemotherapy, can provide synergistic effects, further improving treatment outcomes and overcoming drug resistance.

Data availability

The data is available upon reasonable request.

Conflicts of interest

There are no conflicts to declare.

Acknowledgements

This work was supported by funds from the Spanish Ministerio de Ciencia, Innovación e Universidades and Agencia Estatal de Investigación (MICIU/AEI/10.13039/501100011033) (PID2020-117508RB-I00 and PID2023-146161OB-I00 to V. M.; PID2021-122850NB-I00 to J. R.), by "ERDF A way of making Europe" (PID2023-146161OB-I00 to V. M.; PID2021-122850NB-I00 to J. R.), Fundación Séneca-CARM (project 21989/PI/22 to J. R.) and the Fundació "la Caixa" (CaixaImpulse Innovation project LCF/TR/CI23/56000013 to V. M.). COST Action CA22131, LUCES, is acknowledged.

References

1 F. Annunziata, C. Pinna, S. Dallavalle, L. Tamborini and A. Pinto, An Overview of Coumarin as a Versatile and Readily Accessible Scaffold with Broad-Ranging Biological Activities, *Int. J. Mol. Sci.*, 2020, **21**(13), 4618, DOI: **10.3390/ijms21134618**.

2 S. Feng, J. Wang, L. Zhang, Q. Chen, W. Yue, N. Ke and H. Xie, Coumarin-Containing Light-Responsive Carboxymethyl Chitosan Micelles as Nanocarriers for Controlled Release of Pesticide, *Polymers*, 2020, **12**(10), 2268, DOI: **10.3390/polym12102268**.

3 Y.-H. Wang, B. Avula, N. P. D. Nanayakkara, J. Zhao and I. A. Khan, Cassia Cinnamon as a Source of Coumarin in Cinnamon-Flavored Food and Food Supplements in the United States, *J. Agric. Food Chem.*, 2013, **61**(18), 4470–4476, DOI: **10.1021/jf4005862**.

4 M. T. Baltazar, S. Cable, P. L. Carmichael, R. Cubberley, T. Cull, M. Delagrange, M. P. Dent, S. Hatherell, J. Houghton, P. Kukic, H. Li, M.-Y. Lee, S. Malcomber, A. M. Middleton, T. E. Moxon, A. V. Nathanail, B. Nicol, R. Pendlington, G. Reynolds, J. Reynolds, A. White and C. Westmoreland, A Next-Generation Risk Assessment Case Study for Coumarin in Cosmetic Products, *Toxicol. Sci.*, 2020, **176**(1), 236–252, DOI: **10.1093/toxsci/kfaa048**.

5 E. Niro, R. Marzaioli, S. De Crescenzo, B. D'Abrosca, S. Castaldi, A. Esposito, A. Fiorentino and F. A. Rutigliano, Effects of the Allelochemical Coumarin on Plants and Soil Microbial Community, *Soil Biol. Biochem.*, 2016, **95**, 30–39, DOI: **10.1016/j.soilbio.2015.11.028**.

6 A. Lacy, Studies on Coumarins and Coumarin-Related Compounds to Determine Their Therapeutic Role in the Treatment of Cancer, *Curr. Pharm. Des.*, 2004, **10**(30), 3797–3811, DOI: **10.2174/1381612043382693**.

7 H.-L. Qin, Z.-W. Zhang, L. Ravindar and K. P. Rakesh, Antibacterial Activities with the Structure-Activity Relationship of Coumarin Derivatives, *Eur. J. Med. Chem.*, 2020, **207**, 112832, DOI: **10.1016/j.ejmech.2020.112832**.

8 F. Dentali, W. Ageno and M. Crowther, Treatment of Coumarin–associated Coagulopathy: A Systematic Review and Proposed Treatment Algorithms, *J. Thromb. Haemostasis*, 2006, **4**(9), 1853–1863, DOI: **10.1111/j.1538-7836.2006.01986.x**.

9 K. N. Venugopala, V. Rashmi and B. Odhav, Review on Natural Coumarin Lead Compounds for Their Pharmacological Activity, *BioMed Res. Int.*, 2013, 2013, (1), 963248, DOI: **10.1155/2013/963248**.

10 M. Lončarić, D. Gašo-Sokač, S. Jokić and M. Molnar, Recent Advances in the Synthesis of Coumarin Derivatives from Different Starting Materials, *Biomolecules*, 2020, **10**(1), 151, DOI: **10.3390/biom10010151**.

11 E. G. Richard, The Science and (Lost) Art of Psoralen Plus UVA Phototherapy, *Dermatol. Clin.*, 2020, **38**(1), 11–23, DOI: **10.1016/j.det.2019.08.002**.

12 A. Onder and A. Trendafilova, A Review on Anomalin: A Natural Bioactive Pyranocoumarin from the Past to the Future, *Chem. Biodiversity*, 2022, **19**(9), e202200167, DOI: **10.1002/cbdv.202200167**.

13 J. Grover and S. M. Jachak, Coumarins as Privileged Scaffold for Anti-Inflammatory Drug Development, *RSC Adv.*, 2015, **5**(49), 38892–38905, DOI: **10.1039/C5RA05643H**.

14 C. Ding and T. Ren, Near Infrared Fluorescent Probes for Detecting and Imaging Active Small Molecules, *Coord. Chem. Rev.*, 2023, **482**, 215080, DOI: **10.1016/j.ccr.2023.215080**.

15 B. Das and P. Gupta, Di(2-Picolyl)Amine Appended Luminescent Probes: Advances in Bioimaging and Therapeutics, *Coord. Chem. Rev.*, 2025, **522**, 216209, DOI: **10.1016/j.ccr.2024.216209**.

16 F. Wang, K. Wang, Q. Kong, J. Wang, D. Xi, B. Gu, S. Lu, T. Wei and X. Chen, Recent Studies Focusing on the Development of Fluorescence Probes for Zinc Ion, *Coord. Chem. Rev.*, 2021, **429**, 213636, DOI: **10.1016/j.ccr.2020.213636**.

17 D. Khan and Shaily, Coumarin-Based Fluorescent Sensors, *Appl. Organomet. Chem.*, 2023, **37**(7), e7138, DOI: **10.1002/aoc.7138**.

18 D. Gupta, E. Guliani and K. Bajaj, Coumarin—Synthetic Methodologies, Pharmacology, and Application as Natural Fluorophore, *Top. Curr. Chem.*, 2024, **382**(2), 16, DOI: **10.1007/s41061-024-00462-z**.

19 S. B. Yadav, Y. Erande, M. C. Sreenath, S. Chitrambalam, I. H. Joe and N. Sekar, Pyrene Based NLOphoric D–π-A-π-D

Coumarin-Chalcone and Their Red Emitting OBO Difluoride Complex: Synthesis, Solvatochromism, Z-Scan, and Detailed TD-DFT Studies, *ChemistrySelect*, 2019, **4**(35), 10385–10400, DOI: **10.1002/slct.201901948**.

20 K. Zheng, H. Chen, S. Fang and Y. Wang, A Ratiometric Fluorescent Probe Based on a Bodipy-Coumarin Conjugate for Sensing of Nitroxyl in Living Cells, *Sens. Actuators, B*, 2016, **233**, 193–198, DOI: **10.1016/j.snb.2016.04.053**.

21 Y. Zhang, N. Song, Y. Li, Z. Yang, L. Chen, T. Sun and Z. Xie, Comparative Study of Two Near-Infrared Coumarin–BODIPY Dyes for Bioimaging and Photothermal Therapy of Cancer, *J. Mater. Chem. B*, 2019, **7**(30), 4717–4724, DOI: **10.1039/C9TB01165J**.

22 C. Duangkamol, P. Muangsopa, S. Rattanopas, P. Wongsuwan, T. Khrootkaew, P. Chueakwon, N. Niamnont, K. Chansaenpak and A. Kamkaew, Polarity and Viscosity-Sensitive Fluorescence Probes for Lipid Droplet Imaging in Cancer Cells, *Dyes Pigm.*, 2023, **216**, 111365, DOI: **10.1016/j.dyepig.2023.111365**.

23 M. J. Matos, L. Santana, E. Uriarte and F. Borges, Thiocoumarins: From the Synthesis to the Biological Applications, *Molecules*, 2022, **27**(15), 4901, DOI: **10.3390/molecules27154901**.

24 J. Kaufmann, J. Wolf and A. Heckel, Extending the Palette of Green Coumarin Photocages – Oligonucleotide Fragmentation and Superior 5′-Caps, *Chem. – Eur. J.*, 2023, **29**(30), e202300390, DOI: **10.1002/chem.202300390**.

25 A. Gandioso, M. Palau, A. Nin-Hill, I. Melnyk, C. Rovira, S. Nonell, D. Velasco, J. García-Amorós and V. Marchán, Sequential Uncaging with Green Light Can Be Achieved by Fine-Tuning the Structure of a Dicyanocoumarin Chromophore, *ChemistryOpen*, 2017, **6**(3), 375–384, DOI: **10.1002/open.201700067**.

26 A. Gandioso, R. Bresolí-Obach, A. Nin-Hill, M. Bosch, M. Palau, A. Galindo, S. Contreras, A. Rovira, C. Rovira, S. Nonell and V. Marchán, Redesigning the Coumarin Scaffold into Small Bright Fluorophores with Far-Red to Near-Infrared Emission and Large Stokes Shifts Useful for Cell Imaging, *J. Org. Chem.*, 2018, **83**(3), 1185–1195, DOI: **10.1021/acs.joc.7b02660**.

27 A. Gandioso, M. Palau, R. Bresolí-Obach, A. Galindo, A. Rovira, M. Bosch, S. Nonell and V. Marchán, High Photostability in Nonconventional Coumarins with Far-Red/NIR Emission through Azetidinyl Substitution, *J. Org. Chem.*, 2018, **83**(19), 11519–11531, DOI: **10.1021/acs.joc.8b01422**.

28 A. Rovira, M. Pujals, A. Gandioso, M. López-Corrales, M. Bosch and V. Marchán, Modulating Photostability and Mitochondria Selectivity in Far-Red/NIR Emitting Coumarin Fluorophores through Replacement of Pyridinium by Pyrimidinium, *J. Org. Chem.*, 2020, **85**(9), 6086–6097, DOI: **10.1021/acs.joc.0c00570**.

29 E. Izquierdo-García, A. Rovira, J. Forcadell, M. Bosch and V. Marchán, Exploring Structural–Photophysical Property Relationships in Mitochondria-Targeted Deep-Red/NIR-Emitting Coumarins, *Int. J. Mol. Sci.*, 2023, **24**(24), 17427, DOI: **10.3390/ijms242417427**.

30 A. Rovira, A. Gandioso, M. Goñalons, A. Galindo, A. Massaguer, M. Bosch and V. Marchán, Solid-Phase Approaches for Labeling Targeting Peptides with Far-Red Emitting Coumarin Fluorophores, *J. Org. Chem.*, 2019, **84**(4), 1808–1817, DOI: **10.1021/acs.joc.8b02624**.

31 E. Izquierdo, M. López-Corrales, D. Abad-Montero, A. Rovira, G. Fabriàs, M. Bosch, J. L. Abad and V. Marchán, Fluorescently Labeled Ceramides and 1-Deoxyceramides: Synthesis, Characterization, and Cellular Distribution Studies, *J. Org. Chem.*, 2022, **87**(24), 16351–16367, DOI: **10.1021/acs.joc.2c02019**.

32 E. Ortega-Forte, A. Rovira, A. Gandioso, J. Bonelli, M. Bosch, J. Ruiz and V. Marchán, COUPY Coumarins as Novel Mitochondria-Targeted Photodynamic Therapy Anticancer Agents, *J. Med. Chem.*, 2021, **64**(23), 17209–17220, DOI: **10.1021/acs.jmedchem.1c01254**.

33 J. Bonelli, E. Ortega-Forte, A. Rovira, M. Bosch, O. Torres, C. Cuscó, J. Rocas, J. Ruiz and V. Marchán, Improving Photodynamic Therapy Anticancer Activity of a Mitochondria-Targeted Coumarin Photosensitizer Using a Polyurethane–Polyurea Hybrid Nanocarrier, *Biomacromolecules*, 2022, **23**(7), 2900–2913, DOI: **10.1021/acs.biomac.2c00361**.

34 V. Novohradsky, A. Rovira, C. Hally, A. Galindo, G. Vigueras, A. Gandioso, M. Svitelova, R. Bresolí-Obach, H. Kostrhunova, L. Markova, J. Kasparkova, S. Nonell, J. Ruiz, V. Brabec and V. Marchán, Towards Novel Photodynamic Anticancer Agents Generating Superoxide Anion Radicals: A Cyclometalated IrIII Complex Conjugated to a Far-Red Emitting Coumarin, *Angew. Chem., Int. Ed.*, 2019, **58**(19), 6311–6315, DOI: **10.1002/anie.201901268**.

35 V. Novohradsky, L. Markova, H. Kostrhunova, J. Kasparkova, J. Ruiz, V. Marchán and V. Brabec, A Cyclometalated IrIII Complex Conjugated to a Coumarin Derivative Is a Potent Photodynamic Agent against Prostate Differentiated and Tumorigenic Cancer Stem Cells, *Chem. – Eur. J.*, 2021, **27**(33), 8547–8556, DOI: **10.1002/chem.202100568**.

36 E. Ortega-Forte, A. Rovira, M. López-Corrales, A. Hernández-García, F. J. Ballester, E. Izquierdo-García, M. Jordà-Redondo, M. Bosch, S. Nonell, M. D. Santana, J. Ruiz, V. Marchán and G. Gasser, A Near-Infrared Light-Activatable Ru(Ii)-Coumarin Photosensitizer Active under Hypoxic Conditions, *Chem. Sci.*, 2023, **14**(26), 7170–7184, DOI: **10.1039/D3SC01844J**.

37 A. Rovira, E. Ortega-Forte, C. Hally, M. Jordà-Redondo, D. Abad-Montero, G. Vigueras, J. I. Martínez, M. Bosch, S. Nonell, J. Ruiz and V. Marchán, Exploring Structure–Activity Relationships in Photodynamic Therapy Anticancer Agents Based on Ir(III)-COUPY Conjugates, *J. Med. Chem.*, 2023, **66**(12), 7849–7867, DOI: **10.1021/acs.jmedchem.3c00189**.

38 E. Ortega-Forte, A. Rovira, P. Ashoo, E. Izquierdo-García, C. Hally, D. Abad-Montero, M. Jordà-Redondo, G. Vigueras, A. Deyà, J. L. Hernández, J. Galino, M. Bosch,

M. E. Alberto, A. Francés-Monerris, S. Nonell, J. Ruiz and V. Marchan, Achieving Red-Light Anticancer Photodynamic Therapy under Hypoxia Using Ir(III)-COUPY Conjugates, *Inorg. Chem. Front.*, 2025, **12**, 3367–3383, DOI: **10.1039/D4QI03369H**.

39 D. Abad-Montero, A. Gandioso, E. Izquierdo-García, S. Chumillas, A. Rovira, M. Bosch, M. Jordà-Redondo, D. Castaño, J. Bonelli, V. V. Novikov, A. Deyà, J. L. Hernández, J. Galino, M. E. Alberto, A. Francés-Monerris, S. Nonell, G. Gasser and V. Marchán, Ruthenium (II) Polypyridyl Complexes Containing COUBPY Ligands as Potent Photosensitizers for the Efficient Phototherapy of Hypoxic Tumors, *J. Am. Chem. Soc.*, 2025, **147**(9), 7360–7376, DOI: **10.1021/jacs.4c15036**.

40 T. C. Pham, V.-N. Nguyen, Y. Choi, S. Lee and J. Yoon, Recent Strategies to Develop Innovative Photosensitizers for Enhanced Photodynamic Therapy, *Chem. Rev.*, 2021, **121**(21), 13454–13619, DOI: **10.1021/acs.chemrev.1c00381**.

41 T. E. Kim and J.-E. Chang, Recent Studies in Photodynamic Therapy for Cancer Treatment: From Basic Research to Clinical Trials, *Pharmaceutics*, 2023, **15**(9), 2257, DOI: **10.3390/pharmaceutics15092257**.

42 Y. Zhang, B.-T. Doan and G. Gasser, Metal-Based Photosensitizers as Inducers of Regulated Cell Death Mechanisms, *Chem. Rev.*, 2023, **123**(16), 10135–10155, DOI: **10.1021/acs.chemrev.3c00161**.

43 B. Mansoori, A. Mohammadi, M. Amin Doustvandi, F. Mohammadnejad, F. Kamari, M. F. Gjerstorff, B. Baradaran and M. R. Hamblin, Photodynamic Therapy for Cancer: Role of Natural Products, *Photodiagn. Photodyn. Ther.*, 2019, **26**, 395–404, DOI: **10.1016/j.pdpdt.2019.04.033**.

44 X. Xiao, K. Ye, M. Imran and J. Zhao, Recent Development of Heavy Atom-Free Triplet Photosensitizers for Photodynamic Therapy, *Appl. Sci.*, 2022, **12**(19), 9933, DOI: **10.3390/app12199933**.

45 Z. Chen, F. Han, Y. Du, H. Shi and W. Zhou, Hypoxic Microenvironment in Cancer: Molecular Mechanisms and Therapeutic Interventions, *Signal Transduction Targeted Ther.*, 2023, **8**(1), 70, DOI: **10.1038/s41392-023-01332-8**.

46 B. Muz, P. de la puente, F.; Azab and A. K. Azab, The Role of Hypoxia in Cancer Progression, Angiogenesis, Metastasis, and Resistance to Therapy, *Hypoxia*, 2015, 83–92.

47 M. Chowdhury and P. K. Das, Hypoxia: Intriguing Feature in Cancer Cell Biology, *ChemMedChem*, 2024, **19**(9), e202300551, DOI: **10.1002/cmdc.202300551**.

48 V.-N. Nguyen, S. Heo, C. W. Koh, J. Ha, G. Kim, S. Park and J. Yoon, A Simple Route toward Next-Generation Thiobase-Based Photosensitizers for Cancer Theranostics, *ACS Sens.*, 2021, **6**(9), 3462–3467, DOI: **10.1021/acssensors.1c01391**.

49 Z. Xu, Y. Song and J. Sun, Simultaneous Production of Singlet Oxygen and Superoxide Anion by Thiocarbonyl Coumarin for Photodynamic Therapy, *Spectrochim. Acta, Part A*, 2025, **327**, 125327, DOI: **10.1016/j.saa.2024.125327**.

50 C.-Y. Shih, P.-T. Wang, W.-C. Su, H. Teng and W.-L. Huang, Nanomedicine-Based Strategies Assisting Photodynamic Therapy for Hypoxic Tumors: State-of-the-Art Approaches and Emerging Trends, *Biomedicines*, 2021, **9**(2), 137, DOI: **10.3390/biomedicines9020137**.

51 Y. Wan, L.-H. Fu, C. Li, J. Lin and P. Huang, Conquering the Hypoxia Limitation for Photodynamic Therapy, *Adv. Mater.*, 2021, **33**(48), 2103978, DOI: **10.1002/adma.202103978**.

52 Y. Tang, Y. Li, B. Li, W. Song, G. Qi, J. Tian, W. Huang, Q. Fan and B. Liu, Oxygen-Independent Organic Photosensitizer with Ultralow-Power NIR Photoexcitation for Tumor-Specific Photodynamic Therapy, *Nat. Commun.*, 2024, **15**(1), 1–13, DOI: **10.1038/s41467-024-46768-w**.

53 L. C.-C. Lee and K. K.-W. Lo, Leveraging the Photofunctions of Transition Metal Complexes for the Design of Innovative Phototherapeutics, *Small Methods*, 2024, 2400563, DOI: **10.1002/smtd.202400563**.

54 N. Kitamura, S. Kohtani and R. Nakagaki, Molecular Aspects of Furocoumarin Reactions: Photophysics, Photochemistry, Photobiology, and Structural Analysis, *J. Photochem. Photobiol., C*, 2005, **6**(2), 168–185, DOI: **10.1016/j.jphotochemrev.2005.08.002**.

55 J. J. Serrano-Pérez, M. Merchán and L. Serrano-Andrés, Photoreactivity of Furocoumarins and DNA in PUVA Therapy: Formation of Psoralen–Thymine Adducts, *J. Phys. Chem. B*, 2008, **112**(44), 14002–14010, DOI: **10.1021/jp805523d**.

56 M. Wu, X. Liu, H. Chen, Y. Duan, J. Liu, Y. Pan and B. Liu, Activation of Pyroptosis by Membrane-Anchoring AIE Photosensitizer Design: New Prospect for Photodynamic Cancer Cell Ablation, *Angew. Chem., Int. Ed.*, 2021, **60**(16), 9093–9098, DOI: **10.1002/anie.202016399**.

57 X. Zhao, T. Wang, F. Shang, J. Yan, M. Jiang, X. Zou, G. Li, Z. Song and J. Huang, Coumarin-Quinazolinone Based Photosensitizers: Mitochondria and Endoplasmic Reticulum Targeting for Enhanced Phototherapy via Different Cell Death Pathways, *Eur. J. Med. Chem.*, 2024, **280**, 116990, DOI: **10.1016/j.ejmech.2024.116990**.

58 N. Zhao, Y. Li, W. Yin, J. Zhuang, Q. Jia, Z. Wang and N. Li, Controllable Coumarin-Based NIR Fluorophores: Selective Subcellular Imaging, Cell Membrane Potential Indication, and Enhanced Photodynamic Therapy, *ACS Appl. Mater. Interfaces*, 2020, **12**(2), 2076–2086, DOI: **10.1021/acsami.9b18666**.

59 Y. Shiraishi, M. Nakamura, K. Yamamoto and T. Hirai, Rapid, Selective, and Sensitive Fluorometric Detection of Cyanide Anions in Aqueous Media by Cyanine Dyes with Indolium–Coumarin Linkages, *Chem. Commun.*, 2014, **50**(78), 11583–11586, DOI: **10.1039/C4CC05412A**.

60 M. Yang, K. Li, L. Zhong, Y. Bu, Y. Ni, T. Wang, J. Huang, J. Zhang and H. Zhou, Molecular Engineering to Elevate Reactive Oxygen Species Generation for Synergetic Damage on Lipid Droplets and Mitochondria, *Anal. Chim. Acta*, 2024, **1311**, 342734, DOI: **10.1016/j.aca.2024.342734**.

61 Z. Yang, J. Liu, H. Zhang, M. Liu, M. Liu, Y. Li, Y.-Q. Sun and W. Guo, Conformationally Restrained Coumarin Hemicyanines: Improved Quantum Yields and Potential

Applications in Bioimaging and Photodynamic Therapy, *Sens. Actuators, B*, 2023, **387**, 133832, DOI: 10.1016/j.snb.2023.133832.

62 P. Li, W. Zhang, Y. Wang, J. Tian, D. Shi and H. Xu, A Near-Infrared and Lysosome-Targeted Coumarin-BODIPY Photosensitizer for Photodynamic Therapy against HepG2 Cells, *J. Photochem. Photobiol., A*, 2023, **441**, 114735, DOI: 10.1016/j.jphotochem.2023.114735.

63 S. Monro, K. L. Colón, H. Yin, J. Roque, P. Konda, S. Gujar, R. P. Thummel, L. Lilge, C. G. Cameron and S. A. McFarland, Transition Metal Complexes and Photodynamic Therapy from a Tumor-Centered Approach: Challenges, Opportunities, and Highlights from the Development of TLD1433, *Chem. Rev.*, 2019, **119**(2), 797–828, DOI: 10.1021/acs.chemrev.8b00211.

64 L. C.-C. Lee and K. K.-W. Lo, Luminescent and Photofunctional Transition Metal Complexes: From Molecular Design to Diagnostic and Therapeutic Applications, *J. Am. Chem. Soc.*, 2022, **144**(32), 14420–14440, DOI: 10.1021/jacs.2c03437.

65 A. Zamora, G. Vigueras, V. Rodríguez, M. D. Santana and J. Ruiz, Cyclometalated Iridium(III) Luminescent Complexes in Therapy and Phototherapy, *Coord. Chem. Rev.*, 2018, **360**, 34–76, DOI: 10.1016/j.ccr.2018.01.010.

66 J. Karges, Clinical Development of Metal Complexes as Photosensitizers for Photodynamic Therapy of Cancer, *Angew. Chem., Int. Ed.*, 2022, **61**(5), e202112236, DOI: 10.1002/anie.202112236.

67 G. Vigueras, G. Gasser and J. Ruiz, Breaking the Deep-Red Light Absorption Barrier of Iridium(III)-Based Photosensitizers, *Dalton Trans.*, 2025, **54**(4), 1320–1328, DOI: 10.1039/D4DT03014A.

68 F. J. Ballester, E. Ortega, D. Bautista, M. D. Santana and J. Ruiz, Ru(Ii) Photosensitizers Competent for Hypoxic Cancers via Green Light Activation, *Chem. Commun.*, 2020, **56**(71), 10301–10304, DOI: 10.1039/D0CC02417A.

69 Z. Deng, H. Li, S. Chen, N. Wang, G. Liu, D. Liu, W. Ou, F. Xu, X. Wang, D. Lei, P.-C. Lo, Y. Y. Li, J. Lu, M. Yang, M.-L. He and G. Zhu, Near-Infrared-Activated Anticancer Platinum(IV) Complexes Directly Photooxidize Biomolecules in an Oxygen-Independent Manner, *Nat. Chem.*, 2023, **15**(7), 930–939, DOI: 10.1038/s41557-023-01242-w.

70 Ł. Balewski, S. Szulta, A. Jalińska and A. Kornicka, A Mini-Review: Recent Advances in Coumarin-Metal Complexes With Biological Properties, *Front. Chem.*, 2021, **9**, 781779, DOI: 10.3389/fchem.2021.781779.

71 S. Balcıoğlu, M. O. Karataş, B. Ateş, B. Alıcı and İ. Özdemir, Therapeutic Potential of Coumarin Bearing Metal Complexes: Where Are We Headed?, *Bioorg. Med. Chem. Lett.*, 2020, **30**(2), 126805, DOI: 10.1016/j.bmcl.2019.126805.

72 H. Shi, C. Imberti, G. J. Clarkson and P. J. Sadler, Axial Functionalisation of Photoactive Diazido Platinum(IV) Anticancer Complexes, *Inorg. Chem. Front.*, 2020, **7**(19), 3533–3540, DOI: 10.1039/D0QI00685H.

73 E. M. Bolitho, C. Sanchez-Cano, H. Shi, P. D. Quinn, M. Harkiolaki, C. Imberti and P. J. Sadler, Single-Cell Chemistry of Photoactivatable Platinum Anticancer Complexes, *J. Am. Chem. Soc.*, 2021, **143**(48), 20224–20240, DOI: 10.1021/jacs.1c08630.

74 Z. Deng, N. Wang, Y. Liu, Z. Xu, Z. Wang, T.-C. Lau and G. Zhu, A Photocaged, Water-Oxidizing, and Nucleolus-Targeted Pt(IV) Complex with a Distinct Anticancer Mechanism, *J. Am. Chem. Soc.*, 2020, **142**(17), 7803–7812, DOI: 10.1021/jacs.0c00221.

75 A. K. Yadav, R. Kushwaha, A. A. Mandal, A. Mandal and S. Banerjee, Intracellular Photocatalytic NADH/NAD(P)H Oxidation for Cancer Drug Development, *J. Am. Chem. Soc.*, 2025, **147**(9), 7161–7181, DOI: 10.1021/jacs.4c18328.

76 Z. Fan, J. Xie, T. Sadhukhan, C. Liang, C. Huang, W. Li, T. Li, P. Zhang, S. Banerjee, K. Raghavachari and H. Huang, Highly Efficient Ir(III)-Coumarin Photo-Redox Catalyst for Synergetic Multi-Mode Cancer Photo-Therapy, *Chem. – Eur. J.*, 2022, **28**(3), e202103346, DOI: 10.1002/chem.202103346.

77 C. Huang, C. Liang, T. Sadhukhan, S. Banerjee, Z. Fan, T. Li, Z. Zhu, P. Zhang, K. Raghavachari and H. Huang, *In vitro* and *In vivo* Photocatalytic Cancer Therapy with Biocompatible Iridium(III) Photocatalysts, *Angew. Chem., Int. Ed.*, 2021, **60**, 9474, DOI: 10.1002/anie.202015671.

78 Z. Zhu, L. Wei, Y. Lai, O. W. L. Carter, S. Banerjee, P. J. Sadler and H. Huang, Photocatalytic Glucose-Appended Bio-Compatible Ir(Iii) Anticancer Complexes, *Dalton Trans.*, 2022, **51**(29), 10875–10879, DOI: 10.1039/D2DT01134D.

79 A. K. Yadav, A. Upadhyay, A. Bera, R. Kushwaha, A. A. Mandal, S. Acharjee, A. Kunwar and S. Banerjee, Anticancer Profile of Coumarin 6-Based Ir(Iii) Photocatalysts under Normoxia and Hypoxia by ROS Generation and NADH Oxidation, *Inorg. Chem. Front.*, 2024, **11**(17), 5435–5448, DOI: 10.1039/D4QI01601G.

80 A. K. Yadav, V. Singh, R. Kushwaha, A. Kunwar, B. Koch and S. Banerjee, Anticancer Potential of Polypyridyl-Based Ir(III)-Coumarin 6 Conjugates under Visible Light and Dark, *Inorg. Chem. Commun.*, 2025, **175**, 114184, DOI: 10.1016/j.inoche.2025.114184.

81 T. Sarkar, A. Bhattacharyya, S. Banerjee and A. Hussain, LMCT Transition-Based Red-Light Photochemotherapy Using a Tumour-Selective Ferrocenyl Iron(III) Coumarin Conjugate, *Chem. Commun.*, 2020, **56**(57), 7981–7984, DOI: 10.1039/D0CC03240A.

82 T. Sarkar, A. Kumar, S. Sahoo and A. Hussain, Mixed-Ligand Cobalt(III) Complexes of a Naturally Occurring Coumarin and Phenanthroline Bases as Mitochondria-Targeted Dual-Purpose Photochemotherapeutics, *Inorg. Chem.*, 2021, **60**(9), 6649–6662, DOI: 10.1021/acs.inorgchem.1c00444.

83 J. Dutta, A. Varshini, S. G. Padaga, A. Bera, T. Sarkar, S. Biswas and A. Hussain, Red and NIR Light-Triggered Enhancement of Anticancer and Antibacterial Activities of

Dinuclear Co(Ii)-Catecholate Complexes, *Dalton Trans.*, 2025, **54**(7), 3027–3038, DOI: 10.1039/D4DT03153A.

84 L. T. Todorov and I. P. Kostova, Coumarin-Transition Metal Complexes with Biological Activity: Current Trends and Perspectives, *Front. Chem.*, 2024, **12**, 1–15, DOI: 10.3389/fchem.2024.1342772.

85 V. R. Naina, A. K. Singh, P. Rauthe, S. Lebedkin, M. T. Gamer, M. M. Kappes, A.-N. Unterreiner and P. W. Roesky, Phase-Dependent Long Persistent Phosphorescence in Coumarin-Phosphine-Based Coinage Metal Complexes, *Chem. – Eur. J.*, 2023, **29**(31), e202300497, DOI: 10.1002/chem.202300497.

86 J. Karges, F. Heinemann, M. Jakubaszek, F. Maschietto, C. Subecz, M. Dotou, R. Vinck, O. Blacque, M. Tharaud, B. Goud, E. Viñuelas-Zahínos, B. Spingler, I. Ciofini and G. Gasser, Rationally Designed Long-Wavelength Absorbing Ru(II) Polypyridyl Complexes as Photosensitizers for Photodynamic Therapy, *J. Am. Chem. Soc.*, 2020, **142**(14), 6578–6587, DOI: 10.1021/jacs.9b13620.

87 M.-F. Wang, R. Yang, S.-J. Tang, Y.-A. Deng, G.-K. Li, D. Zhang, D. Chen, X. Ren and F. Gao, In Vivo Realization of Dual Photodynamic and Photothermal Therapy for Melanoma by Mitochondria Targeting Dinuclear Ruthenium Complexes under Civil Infrared Low-Power Laser, *Angew. Chem., Int. Ed.*, 2022, **61**(38), e202208721, DOI: 10.1002/anie.202208721.

88 J. A. Roque III, H. D. Cole, P. C. Barrett, L. M. Lifshits, R. O. Hodges, S. Kim, G. Deep, A. Francés-Monerris, M. E. Alberto, C. G. Cameron and S. A. McFarland, Intraligand Excited States Turn a Ruthenium Oligothiophene Complex into a Light-Triggered Ubertoxin with Anticancer Effects in Extreme Hypoxia, *J. Am. Chem. Soc.*, 2022, **144**(18), 8317–8336, DOI: 10.1021/jacs.2c02475.

89 T. Sainuddin, J. McCain, M. Pinto, H. Yin, J. Gibson, M. Hetu and S. A. McFarland, Organometallic Ru (II) Photosensitizers Derived from π-Expansive Cyclometalating Ligands: Surprising Theranostic PDT Effects, *Inorg. Chem.*, 2016, **55**(1), 83–95, DOI: 10.1021/acs.inorgchem.5b01838.

90 X.-C. Li, Y. Liu, M. S. Liu and A. K.-Y. Jen, Synthesis, Properties, and Application of New Luminescent Polymers with Both Hole and Electron Injection Abilities for Light-Emitting Devices, *Chem. Mater.*, 1999, **11**(6), 1568–1575, DOI: 10.1021/cm990018c.

91 Z. Lv, H. Wei, Q. Li, X. Su, S. Liu, K. Y. Zhang, W. Lv, Q. Zhao, X. Li and W. Huang, Achieving Efficient Photodynamic Therapy under Both Normoxia and Hypoxia Using Cyclometalated Ru(Ii) Photosensitizer through Type I Photochemical Process, *Chem. Sci.*, 2018, **9**(2), 502–512, DOI: 10.1039/C7SC03765A.

92 R. Nomula, X. Wu, J. Zhao and N. R. Munirathnam, Photodynamic Effect of Light-Harvesting, Long-Lived Triplet Excited State Ruthenium(II)-Polyimine-Coumarin Complexes: DNA Binding, Photocleavage and Anticancer Studies, *Mater. Sci. Eng., C*, 2017, **79**, 710–719, DOI: 10.1016/j.msec.2017.05.123.